THE PHOSPHORYLATION OF SERINE 492 OF PERILIPIN A FACILITATES

ATGL-MEDIATED LIPOLYSIS BY CGI-58 INDEPENDENT MECHANISMS

By

MAYDA HERNANDEZ

A thesis submitted to the

Graduate School-New Brunswick

Rutgers, The State University of New Jersey

and

The Graduate School of Biomedical Sciences

University of Medicine and Dentistry of New Jersey

in partial fulfillment of the requirements

for the degree of

Master of Science

Graduate Program in Biochemistry

written under the direction of

Dr. Dawn L. Brasaemle

_____

_____

_____

New Brunswick, New Jersey

January 2014

ABSTRACT OF THE THESIS

The Phosphorylation of Serine 492 of Perilipin A Facilitates ATGL-mediated

Lipolysis by CGI-58 Independent Mechanisms

By MAYDA HERNANDEZ

Thesis Director:

Dr. Dawn L. Brasaemle

Perilipin A is a lipid droplet-associated protein that controls
triacylglycerol storage and hydrolysis in adipocytes. Lipolysis of triacylglycerols by
adipose triglyceride lipase (ATGL) and hormone-sensitive lipase (HSL) is enabled by the
phosphorylation of perilipin A by protein kinase A (PKA) on six serine residues. The
main goal of this study was to understand how phosphorylation of serine 492 of perilipin
A promotes lipolysis by ATGL, with or without the co-activator CGI-58. We used NIH
3T3 CARΔ fibroblasts ectopically expressing mutated variants of perilipin and ATGL
with or without CGI-58. The perilipin variants included wild-type perilipin A, perilipin
with serine 492 mutated to alanine (perilipin S492A), perilipin in which only serine 492
can be phosphorylated (perilipin Not5), and perilipin in which none of the serine residues
within PKA sites can be phosphorylated (perilipin All6). Cells expressing these
perilipins and ATGL, with or without CGI-58, were lipid loaded with radioactive oleate
to label triacylglycerol; lipolysis was assessed by measuring the appearance of
radiolabeled oleate in the culture medium under basal conditions and when lipolysis was
stimulated by the addition of forskolin and isobutylmethylxanthine.

Rates of basal lipolysis were similar in cells expressing all perilipin variants and significantly lower than rates of stimulated lipolysis. Stimulated ATGL-mediated lipolysis was comparable in cells expressing perilipin Not5 and cells expressing wild-type perilipin A, whereas cells expressing perilipin S492A showed decreased rates of lipolysis. Comparable maximal rates of stimulated lipolysis were observed in cells expressing either perilipin Not5 or wild-type perilipin A when both ATGL and CGI-58 were expressed, whereas cells expressing perilipin S492A showed a trend towards reduced lipolysis. We conclude that the phosphorylation of serine 492 of perilipin A is required for maximal lipolysis catalyzed by ATGL. In the absence of serine 492, the phosphorylation of serine residues within PKA sites 1-4 and 6 can also facilitate ATGL-mediated lipolysis, although not to maximal levels. Since similar results were obtained with and without CGI-58, we propose that phosphorylation of serine 492 facilitates lipolysis by a general mechanism that is not dependent on the availability of CGI-58 to activate ATGL.

could not have been more fortunate of having friends like you. To all the other friends I have made here in New Jersey: thank you.

Last but not least, I want to acknowledge the person that held my hand through the entire race to the finish line: my husband, Ernesto Mendez. Besides being a great person and an awesome partner, Ernesto is also a scientist. Thanks for spending many hours doing experiments with me when I needed you. I can't be more proud of you and I know this process would not have been the same without you. I love you Ernesto, and this success is both yours and mine.

TABLE OF CONTENTS

LIST OF FIGURES

LIST OF ABBREVIATIONS

ABHD5 – α/β-hydrolase domain-containing protein 5

ADRP – Adipose differentiation-related protein

ASO – Anti-sense oligonucleotides

ATGL – Adipose triglyceride lipase

BSA – Bovine serum albumin

CAR – Coxsackie and adenovirus receptor

CDS – Chanarin-Dorfman syndrome

CGI-58 – Comparative gene identification 58

CHO – Chinese hamster ovary

CsCl – Cesium chloride

DEUP – diethylumbelliferyl phosphate

DMEM – Dulbecco's modified Eagle medium

DMSO – Dimethyl sulfoxide

ECL – Enhanced chemiluminescence

EDTA – Ethylenediaminetetraacetic acid

FAF BSA – Fatty acid-free bovine serum albumin

FRET – Fluorescence resonance energy transfer

HSL – Hormone-sensitive lipase

IBMX – 3-isobutyl-1-methylxanthine

IgG – Immunoglobulin G

LSB – Laemmli sample buffer

MEFs – Mouse embryonic fibroblasts

MGL – Monoglyceride lipase

NLSD – Neutral lipid storage disorder

PAGE –Polyacrylamide gel electrophoresis

PBS – Phosphate buffered saline

PCR – Polymerase chain reaction

PKA – Protein kinase A

SDS – Sodium dodecyl sulfate

SEM – Standard error mean

siRNA – Small interfering RNA

TBS-T – Tris buffered saline with Tween-20

TLC – Thin layer chromatography

INTRODUCTION

Obesity is a major health problem in the United States. In medical terms, obesity is defined as the excessive accumulation and storage of fat in the body. According to the Center for Disease Control and Prevention, over 35% of United States adults are obese[1]. Another concern with obesity is that it increases the risk of type-2 diabetes, heart disease, hypertension, and stroke, among others (1). A recent study estimated that the national medical care costs of obesity-related illness in adults in the United States is $209.7 billion (2). In an effort to help prevent and treat these diseases, resources are being channeled towards gaining better understanding of energy balance and regulation of lipid metabolism.

Many types of cells have the capacity to store lipids in the form of lipid droplets. These dynamic organelles have been associated with several biological processes such as energy generation, membrane synthesis, molecular signaling and viral replication (3). Lipid droplets consist of a core of esterified neutral lipids, such as triacylglycerols and sterol esters, surrounded by a phospholipid monolayer (Figure 1). This monolayer provides an amphipathic coating compatible with the hydrophobic lipid core and the aqueous exterior. A wide array of proteins, including lipid synthesis enzymes, lipases, membrane trafficking components and structural proteins localize to lipid droplets to regulate the metabolism of lipids stored in the core (4,5). For the purposes of this work, we will focus on the processes that control lipid droplet metabolism in adipose tissue.

Adipose tissue is the main energy reserve in animals. When extra calories are consumed in the diet, they are stored in the form of triacylglycerol within adipocyte lipid

---

[1] http://www.cdc.gov/obesity/data/adult.html
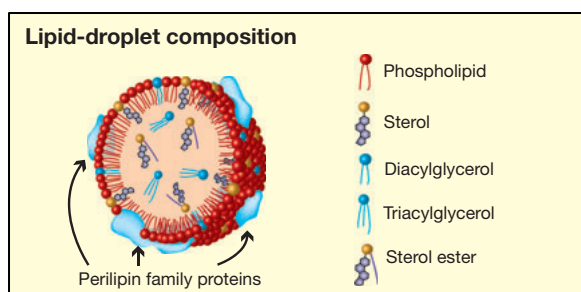
Figure 1. **Structure of lipid droplets**

Lipid droplets are composed of a core of neutral lipids encased by a phospholipid monolayer. Accessory proteins on the surfaces of the droplets regulate lipid synthesis and hydrolysis. Figure reproduced with permission from Guo *et al.,* 2009 (5).

droplets. At times of energy insufficiency, triacylglycerols that have accumulated in adipocyte lipid droplets are catabolized through a hormone-regulated process known as lipolysis. The complete hydrolysis of triacylglycerol results in 3 molecules of fatty acids and 1 molecule of glycerol. Fatty acids can be used by adipocytes for re-esterification to triacylglycerols or phospholipids or they are released into circulation. Albumin-bound fatty acids are carried in the blood to peripheral tissues, where they can serve as substrates for energy production; glycerol is transported to the liver for processes such as gluconeogenesis and triacylglycerol synthesis.

Dysregulation in adipose lipid storage or hydrolysis can lead to serious metabolic problems. For example, high levels of circulating fatty acids coming from increased adipose lipolysis can result in increased import of fatty acids into non-adipose tissues, which have a limited capacity for lipid storage (6). Lipid accumulation beyond a tissue's capacity can cause lipotoxicity, or cell death, in these tissues. Understanding the processes that regulate adipocyte lipid storage and mobilization is therefore important for

the study of lipid-associated disorders. The present work aims to characterize the function of perilipin 1, the major lipid droplet-associated protein in adipocytes, and its regulatory role in the activation of protein kinase A (PKA)-mediated lipolysis.

Lipolysis

Lipid droplets in adipose tissue function as an energy depot. Perilipin 1, a lipid droplet-associated protein, is a key component of the regulation of lipolysis in adipocytes (Figure 2). Under basal or fed conditions, insulin signaling promotes the storage rather than the hydrolysis of triacylglycerols stored in lipid droplets. Perilipin 1 embedded into lipid droplets protects triacylglycerols in the lipid droplet core from the action of cytosolic lipases (7), including the major lipases adipose triglyceride lipase (ATGL) and hormone-sensitive lipase (HSL) (8). At the same time, perilipin 1 binds Comparative Gene Identification-58 (CGI-58), the co-activator of ATGL, at the surfaces of lipid droplets (9). The sequestration of CGI-58 by perilipin 1 prevents CGI-58 from untimely activation of ATGL (10). At times of energy deprivation, such as fasting or exercise, perilipin 1 acts as a scaffold and organizing center for the assembly of the lipolytic machinery (9,11). More than two decades of research have helped to define the major events through which perilipin 1 controls lipolysis.

The lipolytic pathway starts with the binding of catecholamines from the bloodstream and the sympathetic nervous system to β-adrenergic receptors on the plasma membranes of adipocytes (Figure 2). This binding interaction initiates a signaling cascade that leads to the activation of adenylyl cyclase and an increase in intracellular cAMP levels (12). Experimentally, cAMP levels can be increased by use of compounds
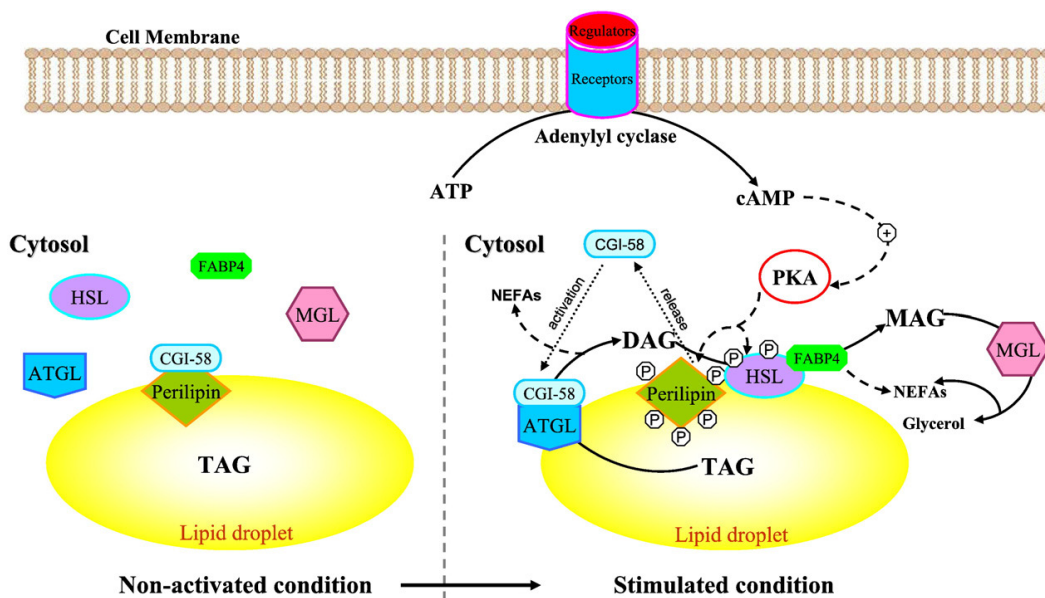
Figure 2. Regulation of lipolysis in adipocytes by perilipin 1.

Perilipin 1 regulates lipolysis in adipocytes in response to hormonal signaling. Under basal conditions, perilipin 1 binds CGI-58 at the surfaces of lipid droplets preventing CGI-58 from interactions and co-activation of ATGL. Perilipin 1 also shields the core triacyglycerols from cytosolic lipases through poorly understood mechanisms. Binding of catecholamines to β-adrenergic receptors on the surfaces of adipocytes leads to an increase in intracellular levels of cAMP and the activation of PKA. Active PKA phosphorylates downstream targets, including perilipin 1 and HSL. The phosphorylation of perilipin A leads to the release of CGI-58 into the cytoplasm where it can interact with ATGL. Phosphorylated perilipin A also facilitates the translocation of phosphorylated HSL to lipid droplets where it docks by binding to perilipin 1. Figure reproduced with permission from Lampidonis *et al.*, 2011 (13). [Reuse license # 3280561044712]

such as forskolin, isoproterenol and isobutylmethylxanthine (IBMX). Forskolin is an adenylyl cyclase activator and isoproterenol is a β-adrenergic receptor agonist. Both compounds work to elevate cAMP levels, although they affect different parts of the lipolytic pathway. IBMX is a phosphodiesterase inhibitor that helps to sustain high levels of cAMP. Increased cAMP levels activate PKA, enabling it to phosphorylate perilipin 1 and HSL (14,15). Phosphorylated HSL can then translocate from the cytosol and dock at the surfaces of lipid droplets in a protein-protein interaction with perilipin 1 to hydrolyze lipid substrates (16,17). Phosphorylation of carboxyl terminal serine residues of perilipin 1 releases CGI-58 from the lipid droplets into the cytosol (9), where CGI-58 then interacts with and co-activates ATGL and presumably recruits the lipase to the surfaces of lipid droplets to catalyze the hydrolysis of triacylglycerols (18,19). Once the lipases gain access to the lipid core, ATGL initiates lipolysis by cleaving triacylglycerols into diacylglycerols, which are further broken down into monoacylglycerols by HSL (20-22). The last step of lipolysis is catalyzed by monoglyceride lipase (MGL), which breaks monoacylglycerols into glycerol and fatty acid (23,24). Fatty acids and glycerol are released into the bloodstream to be utilized by muscle and other tissues. The next pages are dedicated to discussion of this pathway in further detail.

Perilipin 1

In the early 1990's, the lipid metabolism field changed significantly with the discovery of a major phosphoprotein isolated from the fat of rat epididymal adipocytes (25). This protein termed perilipin was the first member of a protein family to be revealed (14). Five genes encode perilipin family proteins, numbered 1-5 in order of discovery (26). Several of the perilipin genes encode multiple protein isoforms. These proteins

comprise the major structural proteins of lipid droplets and are conserved from vertebrates to insects and slime molds (11). Perilipin proteins differ in size, tissue expression, stability and regulation. Of the 5 vertebrate perilipins characterized so far, perilipin 1 is the best-understood family member and the most abundant protein on adipocyte lipid droplets.

Perilipin 1 has 4 proteins isoforms that result from alternative splicing of a single copy gene (27,28). The isoforms are named A, B, C and D. The research described in this thesis investigates the function of perilipin 1A, which will be referred to henceforth as perilipin A. Perilipin A is mainly expressed in adipose tissue and steroidogenic cells of adrenal cortex, ovaries and testes, where it localizes to lipid droplets (29,30). The shorter isoform perilipin 1B can also be found in adipose tissue and steroidogenic cells, while expression of perilipins 1C and 1D is limited to steroidogenic cells (30). To date, perilipin A has been the most studied isoform; little is known about the characteristics or functions of the shorter perilipin isoforms 1B, 1C and 1D.

The functions of perilipin A are intrinsically related to the protein's structural features (Figure 3). Typical to the perilipins, the amino terminus of perilipin A comprises a conserved sequence of 121 amino acids, followed by sequences of 11-mer repeats predicted to form amphipathic α-helices. Central to the protein, 3 hydrophobic sequences have been shown to be necessary and sufficient to direct the targeting of perilipin A to lipid droplets (31,32); these sequences are thought to form hydrophobic hairpins that insert through the phospholipid monolayer and into the neutral lipid core. The carboxyl terminus of perilipin A is unique to perilipin 1 and, together with the amino terminus, provides for the lipid-protective functions of perilipin A (33). Most importantly, perilipin
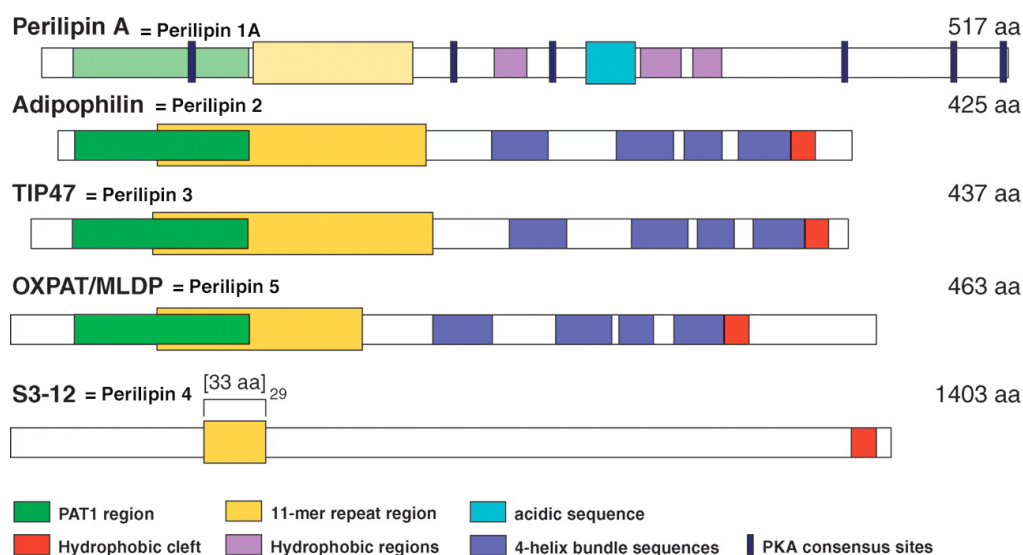
Figure 3. Diagram of structural features of perilipins

The above diagram depicts a structural comparison of the amino acid sequences of mouse perilipins, including perilipin 1A (perilipin A), perilipin 2 (adipophilin), perilipin 3 (TIP47), perilipin 5 (OXPAT/MLDP) and perilipin 4 (S3-12). Colored blocks show regions of sequence similarity, with darker colors indicating the highest similarity. A stretch of approximately 100 residues (depicted in green) is conserved among all of the members of the family except for perilipin 4. The family also shares similar sequences of 11-mer repeats predicted to form amphipathic α-helices (depicted in yellow). Domains predicted to form 4-helix bundles (dark blue) are present in perilipins 2, 3 and 5. A sequence predicted to form a hydrophobic cleft (red) is present in all family members except perilipin 1A. Perilipin 1A is unique in its carboxyl terminal region, which contains an acidic sequence (cyan) between three hydrophobic regions (purple) known to be essential for the targeting of perilipin 1A to lipid droplets. Importantly, perilipin 1A is phosphorylated by PKA on serine residues in at least 6 consensus sequences (charcoal). Figure reproduced with permission from Brasaemle, 2007 (8).

A can be multiply phosphorylated by cAMP dependent protein kinase A (PKA) in the serine residues of at least 6 consensus sites.

The stability of perilipin A is controlled by post-translational mechanisms. A study using Y-1 adrenal cortical cells showed that incubation of these cells with fatty acids and cholesterol dramatically increased triacylglycerol storage within lipid droplets (34). Protein levels of perilipins A and 1C were also increased upon lipid supplementation of these cells, despite a lack of parallel increases in mRNA levels. The increase in protein levels of perilipin A was clearly associated with triacylglycerol synthesis, since incubation of Y-1 cells with the poorly metabolized fatty acid bromopalmitate failed to increase levels of perilipins A and 1C. All of these data support the idea that perilipin A is stabilized when it associates with lipid droplets. Further evidence collected from 3T3-L1 and Chinese hamster ovary (CHO) cells expressing ectopic perilipin A suggests that excess perilipin A that does not associate with lipid droplets undergoes rapid degradation by proteosomal and lysosomal pathways (35,36).

Perilipin A is critical for the control of lipid droplet metabolism. Under fed conditions, perilipin A protects lipid droplets from lipolysis. Brasaemle and co-workers showed that when perilipin A is ectopically expressed in 3T3-L1 fibroblasts, triacylglycerol storage increases 6-30 fold (7). An increase in triacylglycerol content can be due to either increased triacylglycerol synthesis in the cells or decreased hydrolysis of triacylglycerol stores. Experiments measuring triacylglycerol hydrolysis rates in these cells revealed that perilipin A protects adipocyte lipid droplets by decreasing basal triacylglycerol turnover. Thus, this study suggested that the perilipin A coating of lipid droplets acts as a barrier to limit lipase access to the lipids stored in the core. Additional

evidence supporting a role for perilipin A in the protection of adipose triacylglycerol stores came from studies conducted by the Greenberg group. TNF-α is a cytokine that increases lipolysis of adipocyte lipid droplets in part by reducing the expression of endogenous perilipins (37). Adenovirus-mediated overexpression of ectopic perilipin A or 1B in 3T3-L1 adipocytes blocked the increase in lipolysis induced by TNF-α. Moreover, the protein levels of perilipin A or 1B no longer decreased during TNF-α treatment. These data indicate that restoring the perilipin coating of lipid droplets preserves the protein's barrier function and attenuates lipolysis.

Studies conducted in perilipin A knock-out mice revealed that, in addition to its functions in the control of basal lipolysis, perilipin A is necessary to facilitate stimulated lipolysis. The ablation of perilipin A in mice results in leanness from reduced fat mass when compared to wild type mice (38,39). Basal lipolysis in adipocytes of perilipin null mice is increased due to the absence of perilipin A barrier function. Importantly, adipocytes isolated from perilipin null mice failed to increase lipolysis in response to stimulation of β-adrenergic receptors (38,39), indicating that perilipin A is required for maximal lipolytic activity.

In adipocytes, hormone-stimulated lipolysis is modulated by the phosphorylation of perilipin A by PKA. Perilipin A can be phosphorylated on serine residues within at least 6 PKA consensus sequences: Ser 81, Ser 222, Ser 276, Ser 433, Ser 492, and Ser 517. All of these sites are present in rodent perilipin A, but Ser 222 is absent in human perilipin A (8). Mutational studies of serine residues within the PKA sites of perilipin A demonstrated that phosphorylation of different sites selectively regulates lipolysis by different lipases (40). Zhang and colleagues showed that the phosphorylation of one or

more of the first three amino terminal PKA sites of perilipin A facilitates lipolysis by

HSL (40), although later research demonstrated that the phosphorylation of all three sites

is required for HSL-mediated lipolysis (41). The later study showed that the

phosphorylation of serines 81, 222 and 276 leads to the translocation of phosphorylated

HSL from the cytoplasm to lipid droplets and the binding of HSL to amino terminal

sequences of perilipin A (17,41). The protein-protein interaction of HSL and perilipin A

allows the docking of HSL on to the lipid droplet, where it can access the lipid core to

catalyze lipolysis. Zhang and colleagues also showed that phosphorylation of serine

residues within amino (sites 1-3) and carboxyl terminal (sites 4-6) PKA sites of perilipin

A are required for lipolysis catalyzed by non-HSL lipases (40). These findings were

confirmed in subsequent work conducted by Miyoshi and coworkers (42) and Granneman

and coworkers (10) showing that the phosphorylation of the carboxyl terminal PKA sites

5 and 6 of perilipin A are important for maximal ATGL-mediated lipolysis. The

phosphorylation of these sites releases CGI-58 from its binding site on the carboxyl

terminus of perilipin A so that it can interact with and activate ATGL (10). In this thesis,

we investigate in further detail the mechanisms by which the phosphorylation of PKA

site 5 of perilipin A facilitates hormone-stimulated lipolysis.

Altogether, these studies underscore the importance of perilipin A in the control

of adipose lipid metabolism under both basal and stimulated conditions.

Perilipin 2

Perilipin 2, previously known as adipophilin or adipose differentiation-related

protein (ADRP), was the second perilipin to be described and was initially recognized as

a highly induced mRNA during early adipocyte differentiation (43). The expression of perilipin 2 is ubiquitous; it is expressed in all cells and tissues that store neutral lipids in lipid droplets. Like perilipin A, the stability of perilipin 2 is dependent on lipid droplet association (44). Xu and colleagues showed that inhibition of proteasome activity in CHO cells leads to the accumulation of perilipin 2, implying that the degradation of the protein occurs by the ubiquitin-proteasome pathway (45).

Perilipin 2 coats lipid droplets soon after their initial formation in adipocytes, but is eventually replaced by perilipin A as the lipid droplets mature (44). In the absence of perilipin A, perilipin 2 replaces perilipin A coating on lipid droplets, as observed in the adipocytes of perilipin A null mice (39). Yet, perilipin 2 cannot substitute for the function of perilipin A, despite some sequence similarity between the proteins; perilipin 2 is relatively permissive to basal lipolysis and plays no role in facilitating hormonally stimulated lipolysis (41).

For most cells and tissues other than adipocytes, perilipin 2 is the main lipid droplet coat protein (44). Moreover, overexpression of perilipin 2 in cells other than adipocytes, such as COS-7 cells, macrophages and fibroblasts, promotes triacylglycerol storage (46-49). However, when perilipin A is expressed in tissues that normally cover their droplets with perilipin 2, perilipin A displaces perilipin 2 (50). Tansey and colleagues reported that ectopic expression of perilipin A in lipid-loaded CHO cells resulted in perilipin A-coated lipid droplets and decreased levels of perilipin 2. Thus, these findings provide evidence of a competitive relationship between perilipin A and perilipin 2 for binding to lipid droplets.

Two mouse models have been used to study the properties and functions of perilipin 2. The first perilipin 2 knockout mouse created by the Chan lab presented normal adipose metabolism, suggesting that expression of perilipin 2 is not essential for adipose tissue function (51). However, this mouse was later shown to express a truncated form of perilipin 2 (52). A true perilipin 2 knockout mouse model was recently described by McManaman and co-workers (53), who showed that the mice were protected from high-fat diet-induced obesity. Perilipin 2 null mice that were fed a high-fat diet for 8-12 weeks gained significantly less weight than wild-type mice. Perilipin 2 null mice were also resistant to liver steatosis and non-alcoholic fatty liver disease (NAFLD) in response to high-fat feeding (53). Moreover, the subcutaneous white adipose tissue of perilipin 2 null mice exhibited characteristics typical of brown adipose tissue, including multilocular lipid droplets and increased expression of uncoupling protein 1 (UCP1). Thus, this study provides evidence that perilipin 2 is indeed important for the regulation of whole body energy homeostasis.

Data from an additional perilipin 2-deficient mouse model generated by the injection of anti-sense oligos (ASO) into leptin deficient obese mice or diet-induced obese mice support a role for perilipin 2 in the control of lipid metabolism. In this study, ASO injections resulted in decreased perilipin 2 expression in liver, but not in adipose tissue or muscle. Perilipin 2-deficient mice showed suppression of hepatic lipogenic genes, increased insulin sensitivity, and decreased hepatic triacylglycerol content and secretion (54). These studies provide agreement that perilipin 2 is important for normal lipid metabolism in liver. Without a doubt, further experiments are necessary to clarify the roles of perilipin 2 in tissue lipid homeostasis.

Perilipins 3, 4 and 5

Three additional members of the perilipin family, perilipin 3 (formerly, tail-interacting protein 47 (TIP47)), perilipin 4 (formerly, S3-12) and perilipin 5 (formerly, OXPAT (PAT protein expressed in oxidative tissues)) are lipid droplet-associated proteins (8,11,26). Like perilipin 2, perilipin 3 is ubiquitously expressed. Perilipin 4 is expressed primarily in white adipose tissue. Perilipin 5 is expressed in oxidative tissues such as heart, muscle and brown adipose tissue (55-57).

Perilipins 3 and 4 are distinct in that they are stable both in the cytosol and when associated with lipid droplets. Perilipin 3, a protein originally described as part of the mannose-6 phosphate receptor trafficking pathway (58), is mainly associated with newly formed lipid droplets in adipocytes (59). Of all of the perilipins, perilipin 3 is the only family member for which a partial structure has been solved (60,61). The carboxyl terminal 60% of perilipin 3 consists of an α/β domain and an amphipathic four-helix bundle, which forms an "L"-shaped structure (60). While the α/β domain of perilipin 3 could not be compared to the α/β domain of other proteins, the four-helix bundle of perilipin 3 showed high similarity to the four-helix bundle domain formed by the amino terminus of soluble apolipoprotein E (60). Apolipoprotein E is a soluble apolipoprotein that can exist in a lipoprotein-bound and a soluble state. Structural and biophysical studies of apolipoprotein E suggest that the four-helix bundle in soluble apolipoprotein E opens during lipid binding to embed into the phospholipid monolayers of lipoproteins (62). In a similar way, perilipin 3 translocates from the cytosol to nascent lipid droplets during lipid droplet formation (59,63). Hence, the four-helix bundle of perilipin 3 may function similarly to apoliporotein E; opening of the bundle may allow the association of

perilipin 3 with the lipid droplet. Additionally, the closing and opening of the four-helix bundle could explain the stability of perilipin 3 in both the cytosolic and lipid droplet compartments.

Another important characteristic of perilipin 3 is that it can functionally compensate for the absence of perilipin 2 in non-adipose cells (64,65). Sztalryd and colleagues showed that embryonic fibroblasts from perilipin 2 null mice accumulate perilipin 3-coated lipid droplets in response to lipid loading (64). An increase in perilipin 3-coated lipid droplets was also observed in AML12 hepatoma cells when perilipin 2 had been knocked down with siRNA (65). Furthermore, cells with perilipin 3-coated lipid droplets and perilipin 2-coated lipid droplets showed similar lipolysis and fatty acid incorporation into triacylglycerols (64). These results indicate that perilipin 3 can effectively serve the function of perilipin 2. On the other hand, knockdown of perilipin 3 by siRNA in perilipin 2 null embryonic fibroblasts decreased lipid droplet formation in response to fatty acid supplementation (64). Analysis of lipid content in these cells showed that exogenous fatty acids were utilized for phospholipid synthesis more than for triacylglycerol synthesis (64), suggesting that in the absence of perilipin 2 and perilipin 3, synthesis and storage of triacylglycerols is impaired. Overall, these studies show that perilipin 3 and perilipin 2 are important for the control of triacylglycerol storage in non-adipose tissues.

Perilipin 4 is the least studied member of the perilipin family and has the lowest sequence similarity to the rest of the family. Perilipin 4 was first identified as a protein highly expressed during adipocyte differentiation (66). Found primarily in adipocytes of white adipose tissue (67), the major structural feature of perilipin 4 is its multiple tandem

33-mer repeats proposed to form amphipathic helices (68). Multiple immunostaining studies performed by Wolins and colleagues have shown that perilipins 3 and 4, along with perilipin 2, associate in an ordered process with new synthesized triacylglycerol to promote and organize lipid droplet formation and maturation in adipocytes (59,63,67). According to the proposed model, lipid droplets start to form in the periphery of adipocytes; these nascent droplets are coated with perilipin 3 and perilipin 4 (63). As the lipid droplets grow, perilipin 2 increasingly coats the lipid droplets, while the association of perilipins 3 and 4 with lipid droplets decreases (63). Finally, as the lipid droplets mature, perilipin A replaces all other perilipins associated with the lipid droplets. This progression of perilipin proteins suggests that each perilipin makes specific contributions to the coordination of adipocyte lipid droplet formation.

Perilipin 5, previously known as OXPAT, myocardial lipid droplet protein (MLDP) or lipid storage droplet protein 5 (LSDP5), is the most recently described perilipin. Like perilipin A, ectopic expression of perilipin 5 in cultured COS-7 and CHO cells enhances triacylglycerol accumulation by reducing lipolysis (19,55,56). Perilipin 5 directly interacts with ATGL and CGI-58, although not simultaneously (19,69), and can also bind HSL (41). Interestingly, perilipin 5 is protective against lipolysis, even while binding ATGL, CGI-58 and HSL (19,41). Recent studies have found that perilipin 5 is phosphorylated when PKA is activated in cells (19). Thus, it is likely that PKA-mediated phosphorylation of perilipin 5 facilitates lipolysis. Hence, these findings suggest that perilipin 5 protects lipid droplets against lipolysis in the basal state, but also facilitates hormonally stimulated lipolysis by as yet poorly understood mechanisms.

Hormone-Sensitive Lipase

Hormone-sensitive lipase (HSL), the best-characterized adipose lipase, was first identified as an epinephrine-sensitive enzyme in adipose tissue (70,71). HSL is expressed in adipose and steroidogenic tissues, but it can also be found in low quantities in heart, skeletal muscle, macrophages and pancreatic β-cells (72-78). Although the primary enzymatic activity of HSL is thought to be the cleavage of diacylglycerols, HSL can cleave other neutral lipids such as triacylglycerols, cholesteryl esters and retinyl esters (79,80). As its name suggests, HSL responds to hormonal stimuli. Catecholamine signaling in adipocytes results in HSL activation upon phosphorylation by PKA (81). Inversely, insulin signaling inhibits HSL activity through the activation of phosphodiesterase 3B to increase degradation of cAMP, thus reducing the activation of PKA and phosphorylation of downstream targets (24,82).

PKA-mediated phosphorylation of HSL is required for the activation of lipolysis, triggering the translocation of the lipase from the cytosol to the surfaces of lipid droplets where it gains access to its lipid substrates (83). Evidence for this translocation has been collected from several cell models using subcellular fractionation and immunofluorescence microscopy (16,17,84,85). Moreover, maximal lipolysis in adipocytes requires that the translocation and docking of HSL at the surfaces of lipid droplets is coupled to the phosphorylation of perilipin A. Evidence for this requirement derives from a study from the Greenberg group where a perilipin A variant with mutations in PKA-site serine residues was expressed in acyl CoA synthetase/fatty acid transport protein 1 (ACS1/FATP1)-expressing cells, a cell line with enhanced triacylglycerol accumulation in the presence of exogenous fatty acids (86). Souza and

colleagues showed that forskolin-stimulated lipolysis was significantly reduced in cells expressing the perilipin variant with all PKA-site serine residues mutated relative to that measured for unmodified perilipin when HSL was ectopically expressed in the cells (86). Moreover, the translocation of HSL to lipid droplets in response to isoproterenol stimulation was observed in adipocytes differentiated from wild type mouse embryonic fibroblasts (MEFs), but not in adipocytes derived from perilipin-null mice, which have perilipin 2-coated lipid droplets (17). This study indicates that the expression and phosphorylation of perilipin A is essential for maximal HSL-mediated lipolysis in adipocytes. Later work revealed that the phosphorylation of perilipin A is necessary for the binding of phosphorylated HSL to amino terminal sequences of perilipin A, which in turn facilitates lipolysis catalyzed by HSL (41).

Three HSL-deficient mouse models have been reported in the literature so far. Data from these studies revealed that the absence of hormone-sensitive lipase in mice is linked to reproductive defects and the accumulation of diacylglycerol in adipose tissue (20,87,88). In the first 2 models reported, HSL-null male mice exhibited sterility, small size testes, low sperm counts, and vacuolation of epithelial cells (87,88). Intriguingly, Osuga and colleagues did not find any other major differences in the animals' weight or adipose tissue mass relative to wild-type mice (87), suggesting that HSL is dispensable in adipose tissue. In their conclusion, the authors speculated that HSL deficiency in these animals may deprive testicular cells of lipid products released by the action of HSL that are necessary for spermatogenesis. Importantly, because no changes were observed in the body weight and white adipose mass of HSL null mice, this study suggested that HSL is

not the only triacylglycerol lipase in adipose tissue, but that another enzyme can compensate the absence of the lipase.

To clarify the role of HSL in the lipolytic pathway, the Zechner group developed another HSL-null mouse model. Examination of the lipid composition of tissues from these animals revealed the accumulation of diacylglycerol in white and brown adipose tissue, skeletal muscle, heart and testis (20). *In vitro* lipase and lipolysis assays using HSL-deficient mouse tissues confirmed diacylglycerol accumulation and a reduction of isoproterenol-stimulated release of free fatty acids from white and brown adipose tissues, testis, liver and muscle. Consistent with previous data (87), no increase in white adipose tissue triacylglycerol content or total fat mass was observed (20). Altogether, these data demonstrate that the absence of HSL interrupts the lipolytic cascade at the level of diacylglycerol cleavage, suggesting that HSL is primarily a diacylglycerol lipase. Importantly, normal triacylglycerol hydrolysis in these animals hinted of the existence of an alternate lipase for the cleavage of triacylglycerols.

Adipose triglyceride lipase

In 2004, three independent groups identified an additional adipose lipase, naming it 3 different names: adipose triglyceride lipase (ATGL), desnutrin and calcium independent phospholipase A2ζ (iPLA2ζ) (89-91). Mammalian ATGL is also called patatin-like phospholipase domain-containing 2 (PNPLA2) in reference to its patatin domain (92), a domain initially described for the patatin protein found in potatoes. ATGL is highly expressed in adipocytes of mice and humans, with increasing expression

observed during adipocyte differentiation. Additionally, low levels of ATGL can be found in most other tissues (89-91,93).

ATGL has 10 times higher affinity for triacylglycerol than for diacylglycerol when assayed in vitro, hence, ATGL is thought to selectively catalyze the first step of triacylglycerol hydrolysis (89). For example, COS-7 cell extracts from cells previously transfected with ATGL hydrolyzed only triacylglycerol substrates and accumulated diacylglycerol products (89). Additionally, when histidine-tagged ATGL was expressed in differentiated 3T3-L1 adipocytes, ATGL was found to be partially associated with lipid droplets with the rest diffusely distributed in the cytoplasm. Basal release of fatty acids and glycerol in these cells increased concomitant with the expression of ATGL (89). Therefore, these studies underscore the substrate-specificity of ATGL, while suggesting a role for ATGL in the catalysis of basal lipolysis.

Genetic ablation of ATGL in mice leads to modestly increased whole body adipose mass, fat cell hypertrophy and triacylglycerol accumulation in many tissues, particularly heart, testis and kidneys (94). Excessive fat deposition in heart resulted in cardiac dysfunction and premature death of ATGL-null mice. Analysis of the lipolytic capacity of ATGL-deficient adipose tissue revealed approximately 75% reduction in free fatty acid and glycerol release after 2 hours of isoproterenol stimulation. These findings indicate that ATGL is critical for the regulation of lipid metabolism in multiple tissues at different levels. For example, heart failure in ATGL null mice suggests that ATGL is essential for cardiac function and that its activity cannot be replaced by other lipases. On the other hand, mild obesity observed in ATGL null mice suggests that although ATGL is important for white adipose tissue metabolism, its activity can be compensated, at least in

part, by other lipases. Overexpression of ATGL in mice adipose tissue attenuated diet-induced obesity, increased lipolysis and decreased total adipose tissue mass (95). Altogether, these data emphasize the physiological role of ATGL in the initiation of triacylglycerol hydrolysis.

The regulation of ATGL activity is less understood than the regulation of HSL activity. In 3T3-L1 adipocytes, ectopic ATGL associates with lipid droplets under both basal and stimulated states (89). Studies suggest that ATGL is a substrate for phosphorylation at several serine residues; consequences of phosphorylation, as well as the kinases involved, are still under study (95,96). Most importantly, the activity of ATGL is increased by comparative gene identification 58 (CGI-58), also called α/β-hydrolase domain-containing protein 5 (ABHD5). As observed by Lass and colleagues, addition of CGI-58 to ATGL-containing COS-7 cell lysates can increase triacylglycerol hydrolase activity by up to 20-fold compared to ATGL-only or HSL-only cell extracts (97). Additionally, co-expression of ATGL and CGI-58 in COS-7 cells decreased intracellular triacylglycerol accumulation; this decrease was not observed when either ATGL or CGI-58 was singly expressed in the cells (97). Hence, these studies indicate that CGI-58 acts as a co-factor to activate the triacylglycerol hydrolase activity of ATGL. A potential negative regulator of ATGL has been recently identified, G(0)/G(1) switch gene 2 (G0S2). G0S2, which is highly expressed in adipose tissue, appears to interact with ATGL to attenuate its hydrolase activity both *in vitro* and *in vivo* (98,99).

Comparative gene identification-58 (CGI-58)

CGI-58 is a lipid droplet-associated protein (9,100,101) identified by a

comparative proteomic approach using the *C. elegans* proteome as a template to identify novel human gene transcripts (102). CGI-58 is expressed in many tissues, including testis, adipose tissue, liver and muscle (97). Classified as a member of the α/β hydrolase family, CGI-58 contains motifs common to the esterase/lipase/thioesterase subfamily. Notably, CGI-58 is distinct in that its putative catalytic triad contains an asparagine residue instead of the usual serine residue present in other α/β hydrolases. Hence, the sequence of CGI-58 suggests that CGI-58 may not function as a lipase. Lass and co-workers later confirmed that CGI-58 does not have intrinsic triacylglycerol hydrolase activity (97).

Mutations in CGI-58 have been associated with Chanarin-Dorfman syndrome (CDS), a rare autosomal recessive disorder (103). First described in the 1970s, CDS is a neutral lipid storage disease (NLSD) characterized by ichthyosis, or scaly skin, and excessive triacylglycerol accumulation in many cells and tissues (104-106). Most patients with this disorder have hepatic steatosis, while some have ataxia, hearing loss and mental retardation. Ablation of CGI-58 in mice caused similar phenotypes, including triacylglycerol accumulation in various tissues, growth retardation, hepatic steatosis and lethal defects in skin barrier development; CGI-58 null mice die within 16 hours after birth (107). To date, 19 CGI-58 mutations have been identified in CDS patients (108). These mutations include deletions, insertions, point mutations, frameshift aberrations and premature stop codons (103,108). It is important to note that CDS is specifically associated with mutations in CGI-58. A similar disorder was described in the late 2000s that is linked to mutations in ATGL. Neutral lipid storage disease with myopathy (NLSDm) is caused by ATGL mutations and is characterized by excessive lipid

accumulation in many cells and tissues, mild to severe myopathy and absence of ichthyosis (109).

After CGI-58 was first associated with CDS, several studies contributed to clarification of the role of CGI-58 in the pathophysiology of CDS. Studies from our group showed that under basal conditions, when PKA is inactive, CGI-58 localizes to the surfaces of lipid droplets in differentiated 3T3-L1 adipocytes by binding to the carboxyl terminus of perilipin A (9). Interestingly, activation of PKA-mediated lipolysis in these cells resulted in the release of CGI-58 from the lipid droplets into the cytosol (9), away from the site where lipolysis occurs. Lass and coworkers observed a 20-fold increase in triacylglycerol hydrolase activity when COS-7 extracts containing CGI-58 were mixed with extracts containing ATGL, but no effect was observed when CGI-58 was added to HSL-containing extracts (97). These results suggested that CGI-58 increases the lipolytic activity of only ATGL. Additionally, triacylglycerol hydrolase activity of mixtures of 3T3-L1 adipocyte cell extracts containing CGI-58 and extracts in which ATGL had been silenced was drastically reduced (97). Thus, these experiments revealed that CGI-58 assists triacylglycerol hydrolysis in adipocytes by activating ATGL.

To understand the involvement of CGI-58 in CDS, Lass and colleagues cloned three different cDNAs encoding human CGI-58 variants previously identified in CDS patients and expressed them in COS-7 cells (97). Triacylglycerol hydrolysis assays of cell extracts containing these CGI-58 variants mixed with ATGL-containing extracts revealed that the mutated variants of CGI-58 fail to stimulate ATGL activity. Moreover, ectopic expression of functional CGI-58 in skin fibroblasts derived from a CDS patient, which normally accumulate high levels of triacylglycerols, reduced excessive triacylglycerol

accumulation in these cells by 51%. Thus, these studies emphasize the importance of CGI-58 for normal cellular metabolism of triacylglycerol and show that mutations in CGI-58 that disable the activation of ATGL cause CDS.

Project rationale, hypothesis and specific aims

LD remodeling events that occur upon chronic stimulation of β-adrenergic receptors have been repeatedly observed in the literature in cultured adipocytes and primary rodent adipocytes (100,110,111). For example, previous studies from our group have shown that, under basal conditions, perilipin-coated lipid droplets of 3T3-L1 adipocytes are large and exhibit a clustered arrangement (Figure 4). These big droplets disappear and disperse microdroplets are observed upon stimulation of β-adrenergic receptors with isoproterenol and IBMX (100,112). Furthermore, incubation of adipocytes with insulin reverses the pattern of dispersed microdroplets to a basal state with the reformation of macro lipid droplets (113). Our group aimed to elucidate the science behind this apparent morphological change and dispersion of lipid droplets. We hypothesized that the observed lipid droplet remodeling was triggered by the phosphorylation of perilipin A by PKA.

To address the hypothesis, Marcinkiewicz and colleagues ectopically expressed perilipin A in 3T3-L1 fibroblasts, which lack endogenous perilipin A but coat lipid droplets with perilipin 2 (112). Consistent with previous observations, the ectopic perilipin A replaced perilipin 2 on droplets and numerous small perilipin A-coated lipid droplets were observed after lipid loading of the cells; however, unlike adipocytes, only tiny lipid droplets were formed and exhibited a clustered arrangement. Incubation of cells
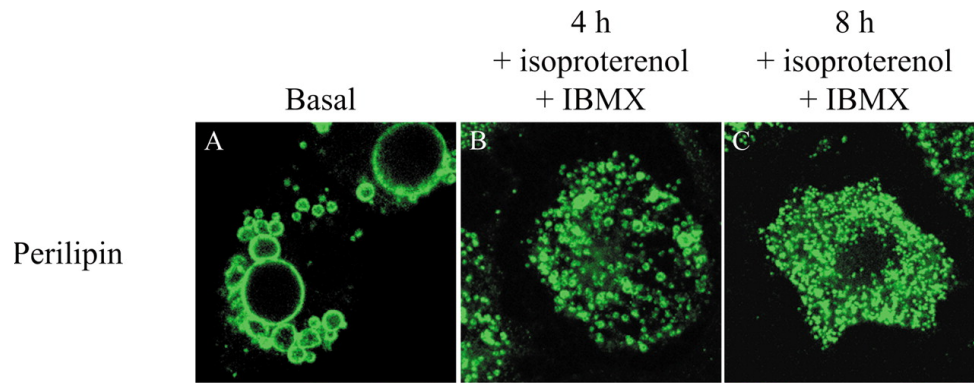
Figure 4. Simulation of lipolysis in 3T3-L1 adipocytes results in lipid droplet remodeling.

Under basal conditions (right panel), staining of perilipin A reveals large and clustered lipid droplets. Incubation of cells with isoproterenol and IBMX causes the appearance of numerous microdroplets dispersed throughout the cytoplasm (middle and left panels). Figure reproduced with permission from Marcinkiewicz *et al.*, 2006 (112).

with forskolin and IBMX resulted in the dispersion of microdroplets throughout the cytoplasm. Immunoblotting of cellular proteins showed that perilipin A was phosphorylated by PKA and that the total mass of perilipin A did not change upon lipolytic stimulation and lipid droplet dispersion. Importantly, lipolysis was not required for lipid droplet dispersion to occur, since stimulation of lipolysis in 3T3-L1 fibroblasts expressing perilipin A in the presence of the serine esterase inhibitor diethylumbelliferyl phosphate (DEUP) inhibited lipolysis but did not impede the process.

To further examine how the PKA-mediated phosphorylation of perilipin A is involved in lipid droplet remodeling, Marcinkiewicz and colleagues made several variants of perilipin A by mutating the serine residues within PKA consensus sites to

alanine either individually or in combination (112). These variants were expressed in 3T3-L1 fibroblasts and analyzed for their effects on lipid droplet morphology and distribution under basal and stimulated conditions. Under basal conditions, all of the perilipin variants promoted the formation of tiny lipid droplets organized in clusters. Under conditions of stimulated lipolysis, lipid droplets coated with unmodified perilipin A dispersed throughout the cytoplasm. However, those variants in which the serine residue in PKA site 5 (Ser 492) was mutated to alanine failed to trigger the dispersion of lipid droplets. Substitution of serine 492 with the phosphomimetic glutamic acid did not support dispersion of lipid droplets in the presence or absence of forskolin and IBMX, suggesting that negative charge is insufficient to trigger lipid droplet dispersion, only phosphate will suffice. Together, these findings suggest that phosphorylation of perilipin serine 492 triggers lipid droplet dispersion in lipolytically stimulated 3T3-L1 fibroblasts.

We hypothesized that dispersion of lipid droplets should facilitate lipolysis by increasing lipase access to lipid droplets. To test whether or not the phosphorylation of perilipin serine 492 had a significant effect on lipolysis, adenoviral expression vectors for the expression of PKA-site variants of perilipin A were prepared. These variants included wild-type perilipin A, a perilipin variant in which all PKA sites are available for phosphorylation except PKA site 5 (perilipin S492A), a perilipin variant in which only PKA site 5 is available to be phosphorylated (perilipin S1234A6E; named perilipin Not5), and a perilipin variant in which all the PKA sites are unavailable for phosphorylation (perilipin S12345A6E; named perilipin All6). These perilipin variants were expressed in NIH 3T3 CARΔ fibroblasts, a cell line that expresses a truncated version of the coxsackie and adenovirus receptor (CAR) (114). Because of this

modification, NIH 3T3 CARΔ fibroblasts have enhanced capacity for adenovirus uptake. Importantly, these cells have no detectable endogenous perilipin A, HSL or ATGL. Cells expressing the perilipin variants were incubated with 600 μM ^{3}H-labeled oleic acid for 12 hours to promote triacylglycerol synthesis and storage, stabilize the perilipin variants, and label the intracellular lipids. Cells were then incubated with forskolin and IBMX to increase intracellular cAMP levels; high cAMP levels results in the activation of PKA and stimulation of lipolysis. The ability of the perilipin variants to facilitate stimulated lipolysis was assessed by measuring the efflux of radiolabeled fatty acid into the media.

Results from these experiments have shown that when ectopic perilipin A is expressed in NIH 3T3 CARΔ cells, phosphorylation of serine 492 alone is sufficient to promote more than 75% of maximal lipolysis relative to wild type perilipin A (Liang and Brasaemle, unpublished data). Hence, these results confirm a role for the phosphorylation of serine 492 of perilipin A in the activation of PKA-mediated lipolysis. However, a limitation of this earlier study was that the endogenous lipases catalyzing lipolysis in NIH 3T3 CARΔ cells were unknown. Thus, in this thesis, we evaluate how the phosphorylation of perilipin A by PKA affects lipolysis in the presence of ectopic ATGL, a major lipase in adipose tissue.

We reasoned that phosphorylation of serine 492 of perilipin A could be driving lipid droplet remodeling and dispersion as a means to facilitate stimulated lipolysis. The appearance of lipid microdroplets was initially proposed to be the result of lipid droplet fragmentation in response to the effect of β-adrenergic agonists. This fragmentation could in turn promote hydrolysis of triacylglycerols by increasing the surface area available for lipases to dock on lipid droplets (100,112). However, recent studies using coherent anti-

Stokes Raman scattering (CARS) microscopy to explore lipid droplet morphology in

3T3-L1 adipocytes have provided data that contrasts with this model (115,116). Two

groups have shown that stimulation of lipolysis in 3T3-L1 adipocytes in the presence of

the acyl-CoA synthetase inhibitor triacsin C inhibits the formation of micro-droplets

(115,116). This finding suggests that the appearance of microdroplets is a result of the

esterification of fatty acids released from lipolysis into triacylglycerols packaged into

new lipid droplets. Data published by other groups are consistent with these results (113).

Moreover, lipid microdroplet formation can be minimized by the inclusion of fatty acid

free albumin in the culture medium to serve as a fatty acid acceptor to promote efflux of

fatty acids released during lipolysis (115). These new findings eliminate the possibility of

lipid droplet fragmentation as a mechanism to facilitate lipolysis in adipocytes. However,

these data do not negate our previous observations in lipolytically stimulated 3T3-L1

fibroblasts incubated with a lipase inhibitor, which show dispersion of small perilipin A-

coated lipid droplets in response to the putative phosphorylation of serine 492. Also, we

are still interested in the question of how phosphorylation of serine 492 of perilipin A

facilitates lipolysis.

Other groups have studied the role of the phosphorylation of serine 492 in

perilipin A PKA site 5 in the activation of lipolysis, but they also suggest that

phosphorylation of serine 517 in PKA site 6 is equally or more important for the

initiation of lipolysis. The Greenberg group expressed variants of perilipin A with

mutations in PKA site serine residues in perilipin null mouse embryonic fibroblasts that

were then differentiated into adipocytes (42). These cells endogenously express both

ATGL and HSL. As expected, the data showed that expression of a perilipin variant in

which serine residues in all 6 PKA sites had been mutated abolishes PKA-stimulated lipolysis. Mutation of serine 492 in PKA site 5 alone led to a 30% reduction in glycerol release following forskolin treatment. These findings are consistent with previous observations by our group for fibroblasts lacking endogenous HSL and ATGL (Liang and Brasaemle, unpublished). Additionally, perilipin null adipocytes expressing a perilipin variant with serine in PKA site 6 mutated to alanine showed complete abrogation of glycerol release, but micro-droplet formation occurred. This suggests that fatty acids were released during lipolysis to support triacylglycerol synthesis and the formation of new lipid droplets but complete lipolysis did not occur, since glycerol was not released. These data suggest a block in lipolysis at either HSL or MGL. Together, these results suggest a role for the phosphorylation of serine 492 in lipolysis, but also suggest that phosphorylation of Ser517 is important for maximal lipolysis. However, one issue that the study done by the Greenberg group does not fully resolve is how the phosphorylation of PKA sites 1-4 contributes to hormone-stimulated lipolysis. In this thesis, we assess the contributions of phosphorylation of serine 492 (perilipin Not5) to lipolysis relative to phosphorylation of the five sites other than serine 492 (perilipin S492A).

The current model for adipocyte lipolysis establishes that, under basal conditions, perilipin A localizes to lipid droplets and binds CGI-58, preventing the co-activation of ATGL, which is also bound to lipid droplets (9). Activation of lipolysis results in the phosphorylation of perilipin A by PKA and the release of CGI-58 from the lipid droplet to bind and co-activate ATGL. Work conducted by Granneman and coworkers investigated the role of phosphorylation of serine residues in PKA sites of perilipin A in the release of CGI-58 from the surfaces of lipid droplets (10). In their study, Granneman

and coworkers measured protein-protein interactions between perilipin A and CGI-58 by fluorescence resonance energy transfer (FRET) analysis. Fluorescently tagged wild-type perilipin A and CGI-58 were expressed in 3T3-L1 fibroblasts followed by incubation of the cells with forskolin and IBMX to activate lipolysis. Simulation of lipolysis in these cells resulted in reduced FRET between perilipin A and CGI-58, suggesting that the interaction between these proteins decreased and CGI-58 was released from perilipin A. FRET measurements in cells expressing variants of perilipin A with individual mutations of PKA site 5 or site 6 showed reduced interactions between perilipin and CGI-58 upon stimulation of lipolysis, indicating the release of CGI-58. However, combined mutations of serine residues in both PKA sites 5 and 6 of perilipin A facilitated sustained FRET between the mutated perilipin and CGI-58 in stimulated cells. This sustained interaction indicates the continued association of perilipin A and CGI-58 and the failure of the mutated perilipin to release CGI-58 into the cytosol. Thus, these results reveal that phosphorylation of both PKA sites 5 and 6 of perilipin A mediates the release of CGI-58. Moreover, mutations of both perilipin PKA sites 5 and 6 reduced the subsequent interaction between CGI-58 and ATGL as measured by luciferase protein complementation. Hence, the release of CGI-58 from perilipin A following the phosphorylation of PKA sites 5 and 6 of perilipin A is a necessary step for the activation of ATGL by CGI-58 and triacylglycerol hydrolysis.

The goal of this thesis is to gain understanding of how the PKA-mediated phosphorylation of serine 492 in the carboxyl terminus of perilipin A affects lipolysis. Although the studies described above have started to address this question, the specific mechanisms by which the phosphorylation of serine 492 triggers lipolysis have not been

fully elucidated. The prevalent model postulates that the carboxyl terminus of perilipin A modulates lipolysis primarily through the binding and release of CGI-58 from the lipid droplet, in turn affecting the availability of CGI-58 to co-activate ATGL. Importantly, this modulation of CGI-58 availability is a mechanism specific for the control of ATGL-mediated lipolysis. However, studies from our group have shown that the phosphorylation of serine 492 in PKA site 5 of perilipin A facilitates lipolysis in cells that lack endogenous CGI-58 and ATGL (Liang and Brasaemle, unpublished). Based on these observations, we then asked two major questions: first, how does the phosphorylation of serine 492 of perilipin A contributes to the activation of lipolysis in the presence of ATGL? Second, is the mechanism by which phosphorylation of serine 492 alters lipolysis solely through the release of CGI-58 for activation of ATGL, or is it a more general mechanism that controls the activity of other lipases?

We hypothesized that the phosphorylation of serine 492 (PKA site 5) of perilipin A can stimulate lipolysis through a general mechanism not limited to the interactions of perilipin A with CGI-58. The specific aims for this thesis were:

a. To test the effects of PKA-mediated phosphorylation of serine 492 (PKA site 5) of perilipin A on lipolysis mediated by ATGL with and without CGI-58. Earlier studies demonstrated that phosphorylation of serine 492 of perilipin A mediates lipolysis by endogenous lipases in NIH 3T3 CARΔ cells. Here we used the same cell model to investigate how the phosphorylation of perilipin A facilitates lipolysis in the presence of ATGL or both ATGL and CGI-58. Adenoviral constructs were prepared to drive the expression of (1) unmodified perilipin A, (2) perilipin S492A, in which PKA sites 1-4 and 6 are available for

phosphorylation, but not site 5, (3) perilipin S1234A6E (Not5), in which only

PKA site 5 is available to be phosphorylated, (4) perilipin S12345A6E (All6), in

which none of the consensus PKA sites are available for phosphorylation, (5)

mouse wild-type ATGL, and (6) mouse wild-type CGI-58. NIH 3T3 CARΔ

fibroblasts expressing the perilipin variants in the presence of ATGL only or

ATGL and CGI-58 were lipid-loaded with tritium-labeled fatty acids for 4 hours

to stabilize the perilipins, promote lipid droplet formation and label

triacylglycerol in lipid droplets. Lipolysis was stimulated by incubation of the

cells with forskolin and IBMX. Fatty acid efflux into the medium under both

basal and stimulated conditions was quantified by liquid scintillation counting.

Comparison of the data from these experiments to data from previous studies

performed in the absence of ATGL and CGI-58 will help reveal the mechanism

by which the phosphorylation of perilipin A regulates lipolysis by ATGL and

other lipases.

b. To assess whether the perilipin A PKA site variants used for the lipolysis

experiments had different effects on fatty acid uptake and esterification into

triacylglycerols during lipid loading incubations. These studies complement

experiments in the previous aim by revealing how the PKA site variants of

perilipin A affect basal lipolysis during lipid-loading to affect the relative

incorporation of fatty acids into triacylglycerols and phospholipids. NIH 3T3

CARΔ cells ectopically expressing (1) the perilipin variants and ATGL, or (2) the

perilipin variants, ATGL and CGI-58, were lipid-loaded with tritium-labeled fatty

acids and harvested after 4 hours of incubation. Lipids from cell pellets were

solvent-extracted and resolved by TLC. Phospholipid and triacylglycerol bands were scraped and quantified by liquid scintillation counting. Total ^{3}H-oleate incorporation and incorporation ratios of triacylglycerol to phospholipid were compared between samples.

c. <u>To confirm that the perilipin A PKA site variants used for the lipolysis experiments successfully targeted to lipid droplets.</u> This experiment was important to demonstrate that the perilipin variants were successfully expressed and that they effectively displaced endogenous perilipin 2 on lipid droplets. Targeting was confirmed by immunofluorescence microscopy of NIH 3T3 CARΔ cells ectopically expressing the perilipin PKA site variants under basal conditions. Lipid droplets were identified by staining with Bodipy 493/503 (117).

d. <u>To examine whether ATGL is expressed in NIH 3T3 CARΔ cells using immunoprecipitation.</u> This experiment was important given that endogenous lipases in our cell model are as yet unidentified and ATGL is a major lipase in adipocytes and other cells and tissues. Proteins from solubilized cell lysates were precipitated with an affinity-purified antibody raised against ATGL and immunoblotted to detect ATGL using the same antibody. NIH 3T3 CARΔ cells ectopically expressing ATGL were included as positive controls.

MATERIALS

Generation of Adenovirus. Oligonucleotides were purchased from Eurofins MWG Operon (Huntsville, AL). All restriction enzymes utilized for subcloning were purchased from New England Biolabs, Inc. (Ipswich, MA). The PureYield™ Plasmid Midiprep System was purchased from Promega (Madison, WI). The MBS Mammalian Transfection Kit, AdEasy™ XL Adenoviral Vector System, QuikChange® II XL Site-Directed Mutagenesis kit, Zero Blunt® PCR Cloning Kit, Platinum® Pfx DNA Polymerase and One Shot® TOP10 chemically competent *E. coli* cells were purchased from Life Technologies (Carlsbad, CA). Pfu Ultra High-Fidelity DNA Polymerase AD was purchased from Agilent Technologies (La Jolla, CA).

Mammalian Cell Culture. Dulbecco's Modified Eagle Medium (DMEM) was purchased from Fisher Scientific, Inc. (Waltham, MA). Bovine calf serum was purchased from Gemini Bio-Products (West Sacramento, CA). Geneticin (G418) was purchased from Gold Biotechnology, Inc. (St. Louis, MO). Penicillin/streptomycin was purchased from Life Technologies (Carlsbad, CA). Fetal bovine serum, dexamethasone, oleic acid, forskolin, 3-isobutyl-1-methylxanthine (IBMX), cesium chloride (CsCl), and dimethyl sulfoxide (DMSO) were purchased from Sigma-Aldrich, Co. (St. Louis, MO). Bovine insulin was purchased from Cell Applications, Inc. (San Diego, CA). Tritium-labeled oleic acid, [9,10-^{3}H(N)], was purchased from Perkin Elmer, Inc. (Boston, MA). Fatty acid-free bovine serum albumin (FAF-BSA) was purchased from US Biological (Swampscott, MA). Triacsin C was purchased from Enzo Life Sciences, Inc. (Farmingdale, NY).

Preparation of Cell Lysates and Immunoblotting. Protease inhibitor cocktail pills were purchased from Roche Diagnostics (Indianapolis, IN). *DC* Protein Assay reagents were purchased from Bio-Rad Laboratories, Inc. (Hercules, CA). Polyclonal rabbit antibody raised against adipose triglyceride lipase (α-ATGL), product #2138, was purchased from Cell Signaling Technology, Inc. (Danvers, MA). Rabbit polyclonal antibodies raised against an amino terminal peptide of perilipin (α-PAT) and perilipin 2 (α-perilipin 2) have been described previously (44,118). A rabbit polyclonal antibody raised against calnexin, product #ADI-SPA-860, was purchased from Enzo Life Sciences, Inc. (Farmingdale, NY). Peroxidase-conjugated goat anti-rabbit and goat anti-mouse antibodies were purchased from Sigma-Aldrich, Co. (St. Louis, MO). Amersham^{TM} ECL^{TM} Western Blotting Analysis System was purchased from GE Healthcare (UK). SuperSignal West Femto Chemiluminescent Substrate was purchased from Thermo Fisher Scientific, Inc. (Middletown, VA).

Immunoprecipitations. Protein A Sepharose beads were purchased from Life Technologies (Carlsbad, CA). Clean-Blot IP Detection Reagent HRP used in place of a secondary antibody was purchased from Thermo Fisher Scientific, Inc. (Middletown, VA). Iodoacetamide, ethanolamine, triethanolamine and dimethyl pimelimidate dihydrochloride (DMP) were purchased from Sigma-Aldrich, Co. (St. Louis, MO). Octylglucopyranoside was obtained from EMD Millipore Corp. (Billerica, MA).

Immunofluorescence Microscopy. Saponin and goat immunoglobulin G (IgG) were purchased from Sigma-Aldrich, Co. (St. Louis, MO). Glycine was purchased from Fisher Scientific, Inc. (Waltham, MA). A solution of 4% paraformaldehyde in PBS was purchased from Affymetrix, Inc. (Cleveland, OH). SlowFade Anti-Fade kit, Bodipy

493/503 and Alexa Fluor 546-conjugated goat anti-rabbit IgG were purchased from Molecular Probes, distributed by Invitrogen (Eugene, OR).

Triacylglycerol Content Measurements. All solvents for lipid extractions were purchased from Sigma-Aldrich, Co. (St. Louis, MO). Infinity^{TM} Triglycerides Liquid Stable Reagent was purchased from Thermo Fisher Scientific, Inc. (Middletown, VA). Silica gel HLF thin layer chromatography (TLC) plates were purchased from Analtech, Inc. (Newark, DE). ScintiVerse BD Cocktail was purchased from Fisher Scientific, Inc. (Waltham, MA).

METHODS

Mammalian Cell Culture. For the generation and amplification of adenoviruses, AD293 human embryonic cells were used. These cells were cultured in DMEM supplemented with 10% fetal bovine serum, 100 units/ml penicillin, and 100 μg/ml streptomycin.

For all other experiments, mouse NIH 3T3 CARΔ fibroblasts were used. NIH 3T3 CARΔ fibroblasts were engineered using retroviral vectors to express a truncated version of the coxsackie and adenovirus receptor (CAR) lacking the cytoplasmic signaling domain (114). This modification provides the cells with an enhanced capacity for adenovirus uptake, and thus, increases expression of ectopic proteins. NIH 3T3 CARΔ cells were cultured in DMEM supplemented with 10% bovine calf serum, 100 units/ml penicillin, and 100 μg/ml streptomycin. To select for cells expressing CARΔ, 800 μg/ml G418 was also added to the media.

All cells were grown at 37°C in a humidified incubator with a 5.5% CO_2 atmosphere.

Generation of Adenovirus. Full-length mouse cDNA for ATGL was amplified from a template provided by Dr. Derek McMahon using polymerase chain reaction (PCR) with *Pfx* DNA polymerase. The 5' (5'-GCCACCGTCGACATGTTCCCGAGGGAA- 3') and 3'(5' -CGATGAGCTCTCAGCAAGGCGGGAGGC- 3') oligonucleotides were utilized as primers for the reaction and were designed to include the restriction sites *Sal I* and *Xho I*, respectively. The amplified DNA product was first ligated into the Zero Blunt vector, followed by its subcloning into the *Sal I* and *Xho I* sites of the pShuttle-CMV vector. The

ligation product was linearized with *Pme I* and transformed into electrocompetent BJ5183-AD-1 *E.coli* for homologous recombination with the pAdEasy adenoviral plasmid. Plasmid DNA from single bacterial colonies was isolated and digested with *Pac I* to select for positive recombinants. The selected recombinant plasmids were transformed into chemically competent TOP 10 *E.coli*. Plasmid DNA was isolated from single bacterial colonies using an endotoxin-free plasmid preparation kit. Purified DNA was digested with *Pac I* for transfection of AD293 cells using the MBS Mammalian Transfection Kit. First generation adenovirus was harvested from infected AD293 cells 7-10 days after transfection. This viral stock was used for infection of AD293 cells and generation of a passage 2 (P2) adenovirus. The process was repeated two more times to obtain a P4 adenovirus stock. Perilipin A adenoviral stocks previously prepared by Deanna Russell and Devon Golem were also amplified to obtain P3 and P4 adenoviruses. All adenoviruses were purified by CsCl ultracentrifugation (119).

P3 adenoviral stocks for β-galactosidase and the perilipin variant S492A, in which the serine in PKA site 5 was substituted with alanine, were previously prepared and purified by Deanna Russell. She also prepared adenoviruses encoding two other perilipin variants: S12345A6E (All6) and S1234A6E (Not5). For the All6 variant, serine residues in PKA sites 1-5 were mutated to alanine and serine in PKA site 6 was substituted with glutamate. For the Not5 variant, serine residues in PKA sites 1-4 were mutated to alanine and serine in PKA site 6 was substituted with glutamate. Purified CGI-58 adenovirus was obtained from Sarah Hassanien.

Adenoviral Transductions. NIH 3T3 CARΔ fibroblasts were seeded on collagen-coated 6-well dishes at a density of 1.87×10^5 cells/well 20-24 hours before transducing

the cells with the corresponding adenoviruses. Uninfected cells and cells infected with

β-galactosidase adenovirus were included as controls. After a 24-hour incubation period,

the virus-containing media were replaced with growth media. Experiments were

conducted approximately 48 hours after the initiation of viral transduction. During the

last 4 hours of this 48-hour period, the cells were incubated with 600 μM oleic acid with

or without tracer levels of tritium-labeled oleic acid complexed to FAF BSA (4:1 molar

ratio) in growth media, according to the experiment being performed.

Determination of Adenoviral Titers for Perilipin A PKA Variants and ATGL.

To determine the viral titers to use for each of the perilipin A, perilipin S492A, perilipin

Not5 and perilipin All6 adenoviruses, NIH 3T3 CARΔ fibroblasts were transduced with

various doses of each adenovirus as described in the previous section. At the end of the

48-hour incubation period, lipid-loading medium was removed and cells were rinsed with

and collected in phosphate buffered saline (PBS). After centrifuging samples at a speed

of 1200 x*g* for 5 minutes at 4ºC, cell pellets were resuspended in hypotonic lysis buffer

[20 mM Tris pH 7.6, 10 mM NaF, 1 mM EDTA, protease inhibitor cocktail, 2% sodium

dodecyl sulfate (SDS)]. Cell extracts were incubated in a bath sonicator with warming to

60ºC and vortexing every 10-15 minutes for 2-4 hours. Protein content of whole cell

lysates was determined using the *DC* protein assay and a lysate volume containing 30 μg

of total protein was prepared for immunoblotting.

ATGL adenoviral titer was determined using a modification of a published

protocol (86). NIH 3T3 CARΔ fibroblasts were transduced with either perilipin A

adenovirus for 24 hours, ATGL adenovirus for 24 hours, or both perilipin A and ATGL

adenoviruses sequentially for 24 hours each. Cells were lipid loaded with 600 μM oleic

acid complexed to FAF BSA (4:1 molar ratio) at 44 hours post transduction. After 4 hours of lipid loading, cells were rinsed with 0.5% FAF BSA in PBS to remove unincorporated oleate. Cells were then scraped into PBS and centrifuged at a speed of 1200 x*g* for 5 minutes at 4ºC to collect the cells. Cell pellets were resuspended in hypotonic lysis buffer without detergents and disrupted by pulling the cell suspension through a 20G needle while keeping the samples on ice. Approximately ¼ of the cell lysate was removed and SDS was added to a final concentration of 2%. Samples were incubated in a bath sonicator warmed up to 60ºC with frequent vortexing and prepared for protein analysis. The remaining ¾ of the samples were transferred to glass tubes for lipid extraction and TAG content analysis, as previously described (120).

Immunoprecipitation. To test for the expression of endogenous ATGL in NIH 3T3 CARΔ cells, immunoprecipitations were performed. Cells transduced with ATGL served as positive controls. After a 48-hour incubation of positive control cells with adenovirus, cells were harvested by scraping them into PBS and centrifuged at a speed of 1200 x*g* for 5 minutes at 4ºC to collect the cells. Cell pellets were then resuspended in 1 mL of non-denaturing lysis buffer (1% Tween 20, 50 mM Tris-HCl, 300 mM NaCl, 50 mM NaF, 5 mM EDTA, 0.02% sodium azide, pH 7.4) and disrupted by probe sonication with a Branson sonicator with a double-step microtip (product # 101-063-212). Cell membranes were centrifuged at 10,000 xg for 5 minutes at 4ºC and the protein content of the cleared supernatant was determined using the DC protein assay.

The day before the cell harvest, protein A-conjugated Sepharose beads were washed several times with wash buffer (0.1% Tween 20, 50 mM Tris-HCl, 300 mM NaCl, 50 mM NaF, 5 mM EDTA, 0.02% sodium azide, pH 7.4) and incubated with α-

ATGL antibody or non-immune control serum IgG overnight. The beads were then washed with 0.2 M triethanolamine, pH 8.9, and incubated for 3 hours at 4ºC followed by 1 hour at room temperature with 0.05 M dimethyl pimelimidate dihydrochloride, pH 8.9, to cross-link the antibodies to the beads. After these incubations, the beads were sequentially washed with 0.2 M triethanolamine, pH 8.9, 0.1 M ethanolamine, pH 8.9, 0.1 M glycine, pH 3.1, and finally non-denaturing lysis buffer prior to incubation with cell lysates.

Volumes containing 1 mg of total protein for each sample were incubated with the cross-linked beads overnight at 4ºC with end-over-end mixing. The beads were then rinsed several times with wash buffer and boiled in 2x LSB for 10 minutes to elute the immunoprecipitated proteins. After boiling, the beads were centrifuged at 100 xg for 1 minute and the cleared supernatant was loaded on to an SDS-PAGE gel for protein separation followed by electrophoretic transfer of proteins to a nitrocellulose membrane.

Immunofluorescence Microscopy. NIH 3T3 CARΔ fibroblasts were transduced with purified adenoviruses corresponding to the PKA sites variants perilipin A, perilipin S492A, perilipin Not5 and perilipin All6. Twenty-four hours later, cells were incubated with 0.25% trypsin-EDTA and re-plated on glass coverslips with a 1:2 dilution. Thirty-six hours post-transduction, cells were incubated with 200 μM oleic acid complexed to FAF BSA (4:1 molar ratio) diluted in growth media. Forty-eight hours post-transduction, cells on coverslips were rinsed with PBS and fixed with 4% paraformaldehyde in PBS for 20 minutes at room temperature.

After extensive rinses with PBS, cells were incubated with a blocker solution containing 0.2 M glycine, 0.1 mg/ml saponin and 0.2 mg/ml goat IgG in PBS for 1 hour

at room temperature to make cells permeable and block non-specific binding sites for

IgGs. The blocked coverslips were transferred individually to wells of a 24-well dish and

probed with α-PAT (1:5,000) antibody in blocker solution overnight at 4°C. Cells were

then incubated for 1 hour at room temperature with goat anti-rabbit Alexa Fluor 546

(1:10,000) in blocker solution to detect perilipin A and simultaneously with Bodipy

493/503 (0.01 mg/ml) to stain neutral lipids. Stained coverslips were mounted on glass

slides using reagent A of the SlowFade Anti-fade kit and sealed with nail polish.

Imaging was performed using a Nikon Eclipse E800 fluorescence microscope and a

Photometrics CoolSNAP *EZ* digital camera. Original images were processed with the

NIS Elements software, captured in black and white and colorized for aesthetic purposes.

    Lipolysis Experiment. NIH 3T3 CARΔ fibroblasts were plated in 6-well cell

culture dishes and transduced with purified adenoviruses corresponding to the PKA sites

variants perilipin A, perilipin S492A, perilipin Not5 and perilipin All6 for 24 hours. For

some experiments, cells were also transduced with purified adenoviruses for the

expression of ATGL with or without CGI-58 for the next 24 hours. During the last 4

hours of the 48-hour incubation, cells were incubated with 600 μM tritium-labeled oleic

acid (5 μCi/well) complexed to FAF BSA (4:1 molar ratio) diluted in growth media. At

the end of this 4 hour incubation, cells were rinsed with 0.5% FAF BSA-PBS to remove

unincorporated oleate. Lipolysis was stimulated in some samples by adding 10 μM

forskolin, 0.5 mM IBMX and 6 μM triacsin C (a long-chain fatty acyl-CoA synthetase

inhibitor) diluted in 3% FAF BSA – DMEM to the cells. For basal conditions, cells were

supplemented with 3% FAF BSA – DMEM with 6 μM triacsin C and dimethyl sulfoxide

(DMSO) as a vehicle control. Media samples (200 μL) were collected at 0, 2, 4, and 6

hours following removal of radiolabeled fatty acids to measure fatty acid release into the media by scintillation counting (PerkinElmer Life Sciences Wallac 1409 Liquid Scintillation Counter).

Within the experimental design, samples were included to evaluate expression of ectopic proteins and radiolabeled lipid uptake into the cells. To assess lipid uptake, a set of cells expressing the different ectopic proteins were lipid-loaded with tritium-labeled oleic acid for 4 hours, rinsed with 0.5% FAF BSA-PBS and harvested by scraping cells into PBS. Samples were centrifuged at a speed of 1200 x*g* for 5 mins at 4ºC to collect the cells and the supernatants were removed. Lipids were extracted from the cell pellets according to the Bligh and Dyer method (121) and separated on a TLC plate using hexane: diethyl ether: formic acid (80:20:2). Resolved lipids were visualized by brief iodine vapor exposure and bands corresponding to triacylglycerol and phospholipids were scraped and prepared for scintillation counting. Samples designated for protein analysis were transduced with the various adenoviruses, incubated with non-radioactive oleic acid, rinsed with PBS and harvested by scraping into PBS. Samples were prepared for protein analysis as described in the section entitles "Determination of Adenoviral Titers for Perilipin A PKA Variants and ATGL" and then subjected to immunoblotting for perilipin A, perilipin 2, and calnexin. For certain experiments, immunoblotting for ATGL and CGI-58 was also performed.

Immunoblotting. Cell lysate volumes corresponding to 30 μg of total protein were diluted in Laemmli sample buffer (LSB) and boiled for 5 minutes (122). Proteins in samples were separated in a 10% denaturing sodium dodecyl sulfate-polyacrylamide gel (SDS-PAGE) and then transferred to a nitrocellulose membrane by electrophoresis. The

membrane was then blocked with 5% non-fat milk diluted in Tris-Tween buffered saline (TBS-T; 20 mM Tris, 137 mM NaCl, 0.02% Tween-20, pH 7.6).

For detection of perilipin A, perilipin 2 and calnexin, the membrane was incubated overnight with all 3 primary antibodies including α-PAT (1:25,000), α-perilipin 2 (1:50,000), and α-calnexin (1:5,000) diluted in 5% BSA in TBST. Peroxidase-conjugated goat α-rabbit IgG was used as the secondary antibody. To confirm the expression of ATGL, separate gels and membranes were prepared. Membranes were probed with α-ATGL (1:2,000) and α-calnexin (1:5,000) diluted in 5% BSA in TBST. Peroxidase-conjugated goat α-rabbit IgG was used as the secondary antibody. Proteins were visualized by enhanced chemiluminescence (ECL) and X-ray film exposure. Relative signal intensity was determined by densitometry using a Bio-Rad GS-800^{TM} calibrated densitometer and the Bio-Rad Quantity One software.

Statistical Analysis. Data are expressed as the mean ± SEM. Lipolysis data were analyzed by two-way analysis of variance (ANOVA) using Bonferroni test for multiple comparisons (GraphPad Prism). Measurements of the incorporation of radiolabeled fatty acids into triacylglycerols were analyzed by one-way ANOVA using Tukey's test. Significance was set at $p < 0.05$.

RESULTS

Perilipin PKA site variants target to lipid droplets. We hypothesized that the

phosphorylation of serine residues in PKA consensus sequences within the carboxyl

terminus of perilipin A is critical for the regulation of PKA-stimulated lipolysis. In this

study, we are specifically interested in the phosphorylation of serine 492 in PKA site 5.

To test this, members of our group generated several mutated variants of perilipin A by

substituting the serine residues within PKA consensus sequences with alanines in

different combinations. These perilipin variants were expressed in NIH 3T3 CARΔ

fibroblasts, a cell line with enhanced adenovirus uptake, and tested for their ability to

promote lipolysis in response to elevated levels of intracellular cAMP. The PKA site

variants included wild-type perilipin A; perilipin S492A, in which all sites except site 5

can be phosphorylated; perilipin S1234A6E (Not5), in which only PKA site 5 is available

to be phosphorylated; and perilipin S12345A6E (All6), in which all of the consensus

PKA sites have been mutated to prevent phosphorylation. For the perilipin Not5 and All6

variants, the serine in PKA site 6 was mutated to glutamic acid instead of alanine because

variants with alanine substitutions in this position have been shown to be difficult to

express in 3T3-L1 fibroblasts (112). Because serine 517 is the last residue in the

sequence of murine perilipin A, it is likely that this amino acid plays a role in targeting

the protein to lipid droplets for subsequent stabilization of the protein. Previous work

established that perilipin A with substitution of serine 517 with glutamic acid targets to

lipid droplets (112).

To determine whether the perilipin PKA variants target to lipid droplets, an

immunofluorescence microscopy experiment was performed. Previous work had shown

that the targeting of perilipin A to lipid droplets is directed by three central hydrophobic sequences of the protein (32) and is not dependent on perilipin A phosphorylation. Since there are no PKA sites within these sequences, we hypothesized that all of the perilipin variants should target to lipid droplets. NIH 3T3 CARΔ cells were transduced with the various perilipin variants and prepared for immunostaining with an antibody raised against the amino terminus of perilipin A. Lipid droplets were identified using Bodipy 493/503, a fluorescent probe for neutral lipids (117). The appearance of bright rings surrounding lipid droplets showed that each of the perilipin variants localized to lipid droplets under basal conditions when cAMP levels are low and PKA is not activated (Figure 5).

Choosing adenoviral titers for the expression of perilipin A PKA site variants. Before beginning experiments to study the effects of perilipin PKA site mutations, it was necessary to determine the adenoviral titers needed to drive comparable expression of the different variants. Under basal conditions, perilipin A on adipocyte lipid droplets serves as a barrier against lipases and decreases triacylglycerol turnover (7). Thus, we reasoned that differences in protein expression or unequal transduction efficiency among the perilipin PKA site variants could result in unequal perilipin A content of lipid droplets. If this is accompanied by increases in perilipin 2-coated droplets, the measurements of basal and stimulated lipolysis may reflect both the relative content of perilipin A-to-perilipin 2-coated lipid droplets and the effects of the mutations being studied. To minimize these potential complications, various titers of adenoviruses for the perilipin PKA site variants were tested.

Figure 5. Perilipin A PKA-site mutated variants target to lipid droplets in NIH 3T3 CARΔ fibroblasts

NIH 3T3 CARΔ fibroblasts were transduced with adenoviruses to express either wild-type perilipin A or perilipin variants S492A, Not5 or All6. Cells were lipid loaded with 200 µM oleic acid for 12 hours and prepared for staining with perilipin antiserum and Alexa Fluor 546–conjugated secondary antibody (depicted in green). Neutral lipids were stained with Bodipy 493/503 (depicted in red).
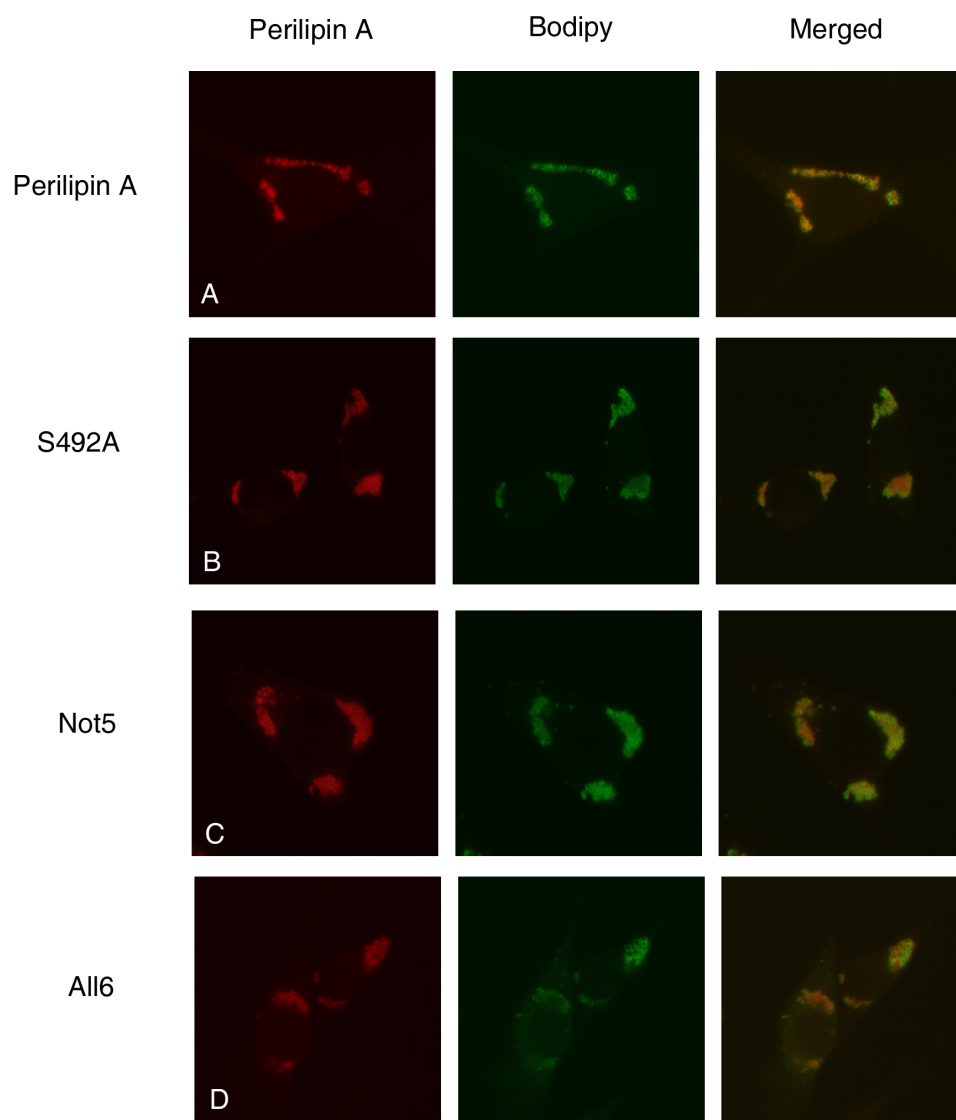
To normalize expression of the perilipin variants, NIH 3T3 CARΔ cells were transduced with different doses of adenoviruses for the perilipin variants and then lipid loaded for the final 12 hours. Cells were harvested 2 days after transduction and lysates were prepared for immunoblotting with antibodies raised against perilipin A, perilipin 2 and calnexin (Figure 6A). Densitometric analysis was used to quantify the relative expression of the perilipin A PKA site variants (Figure 6B). Viral titers that yielded similar levels of protein expression were chosen for subsequent experiments. For example, this experiment suggested that 10 μL of wild-type perilipin A adenovirus would yield similar levels of protein expression as 16 μL of perilipin S492A adenovirus, 14 μL of perilipin All6 adenovirus and 25 μL of perilipin Not5 adenovirus. Adenovirus encoding β-galactosidase was used as a negative control throughout the lipolysis experiments; lipid droplets in β-galactosidase expressing cells are covered with endogenous perilipin 2. The adenoviral titer for β-galactosidase was chosen to avoid cytotoxicity but allow detection of the protein by immunoblotting (not shown).

Perilipin A is stabilized upon binding to lipid droplets (34). In addition, when perilipin A is ectopically expressed in cells that have endogenous perilipin 2, perilipin A displaces perilipin 2 on lipid droplets through a competitive binding process (44,50,86). To efficiently express the perilipin PKA site variants in this experiment, 600 μM oleic acid was added to the culture medium for 12 hours to promote triacylglycerol synthesis and storage in lipid droplets, and hence, stabilize perilipin. However, the immunoblots showed significant expression of endogenous perilipin 2; the expression levels of perilipin 2 in cells expressing the perilipin variants were similar to uninfected cells or cells expressing β-galactosidase (Figure 6A). This suggests that adenoviral expression

Figure 6. Titration of adenovirus doses for perilipin A PKA-site variants in NIH 3T3 CARΔ fibroblasts

NIH 3T3 CARΔ fibroblasts were transduced with different titers of adenoviral vectors for the expression of wild-type perilipin A and perilipin phosphorylation variants S492A, All6 or Not5 for 48 hours. Cells were lipid loaded with 600 µM oleic acid for the final 12 hours before harvesting cells 48 hours after transduction and immunoblotting for perilipin A, perilipin 2 and calnexin (A). Densitometry was performed to calculate each band's volume to determine the viral titers that yielded similar levels of protein expression for each perilipin variant. Data shown in B correspond to the samples marked with an asterisk (*) in (A). Data are representative of two experiments.

(A)
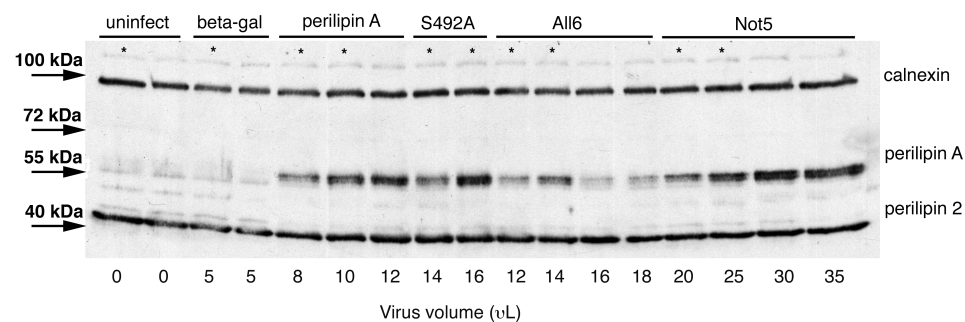
(B)
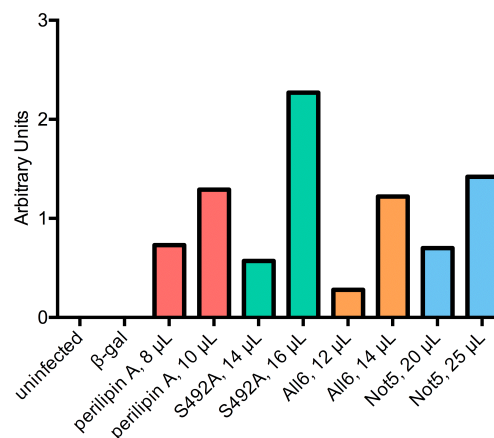
vectors drive a finite level of ectopic perilipin A expression and that lipid loading of cells in excess of the amount needed to stabilize ectopic perilipin A leads to increased levels of perilipin 2- coated lipid droplets. Perilipin 2 is relatively permissive to basal lipolysis and does not respond to the activation of PKA. Thus, for our goal of understanding how the phosphorylation of perilipin A by PKA mediates lipolysis, it was important to optimize the lipid loading conditions to maximize the expression of ectopic perilipin A while minimizing levels of perilipin 2.

Short incubations of NIH 3T3 CARΔ fibroblasts with fatty acids promote maximal expression of ectopic perilipin A. To determine the optimal lipid loading conditions that would maximize levels of ectopic perilipin A while minimizing perilipin 2, NIH 3T3 CARΔ cells were transduced to express wild-type perilipin A and lipid loaded with 600 μM oleate for 0, 2, 4, 6 and 8 hours prior to cell harvest. Densitometric analysis of immunoblots was used to quantify protein levels of perilipin A and perilipin 2 (not shown). Immunoblotting data in Figure 7 show that short incubation times with fatty acids resulted in high levels of ectopic perilipin A with low levels of endogenous perilipin 2. Protein levels of ectopic perilipin A were maximal at 2-4 hours of lipid loading; longer incubations with fatty acids increased levels of perilipin 2-coated lipid droplets. These data suggest that short incubations of cells expressing ectopic perilipin A with fatty acids are sufficient to stabilize the finite amount of perilipin A expressed in the cells without significantly increasing endogenous perilipin 2 expression. Based on these results, an incubation of 4 hours with fatty acids was chosen for subsequent experiments.

Figure 7. Brief incubations of NIH 3T3 CARΔ cells expressing perilipin A with fatty acids maximizes the expression of ectopic perilipin A while minimizing the expression of endogenous perilipin 2

NIH 3T3 CARΔ fibroblasts were transduced with perilipin A adenovirus for 48 hours and then incubated with 600 μM oleic acid for 0, 2, 4, 6 or 8 hours. Cells were harvested and proteins were resolved by SDS-PAGE for immunoblotting with antibodies against perilipin A, perilipin 2 and calnexin.
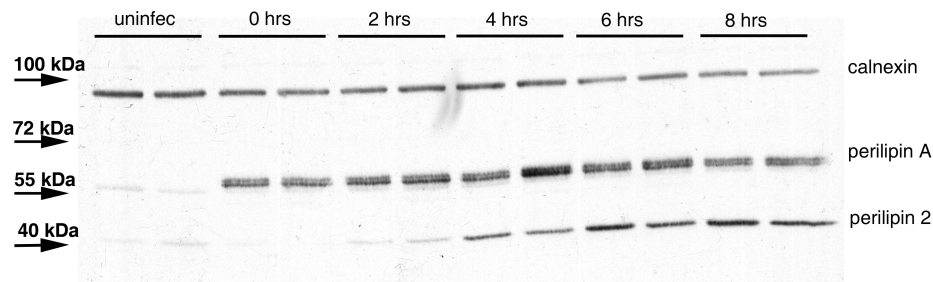
Perilipin A protects lipid droplets against basal lipolysis and increases PKA-stimulated lipolysis in NIH 3T3 CARΔ fibroblasts. For the first lipolysis study, we conducted an experiment to test the experimental conditions that had been established by a previous graduate student. Wild-type perilipin A or the control protein β-galactosidase was expressed in NIH 3T3 CARΔ cells. Forty-four hours after transduction, the cells were incubated for 4 hours with 600 μM ^{3}H-oleic acid complexed to FAF-BSA to incorporate a radioactive tracer into the pool of stored triacylglycerols. To stimulate lipolysis, cells were incubated with 3% FAF BSA-DMEM containing 10 μM forskolin, 0.5 mM IBMX and 6 μM triacsin C. Forskolin is an adenylyl cyclase activator and IBMX acts as a phosphodiesterase inhibitor to sustain elevated levels of cAMP; these compounds assure strong activation of PKA. Triacsin C is an acyl-CoA synthetase inhibitor that blocks the re-esterification of fatty acids released during lipolysis into triacylglycerol. For basal conditions, cells were incubated with 3% FAF BSA-DMEM containing 6 μM triacsin C and DMSO for vehicle control. Lipolysis was estimated from the appearance of radiolabeled oleic acid in the media during the next 6 hours. Media samples were collected at 0, 2, 4 and 6 hours and analyzed by liquid scintillation counting.

For these experiments, control cells were transduced with β-galactosidase. Since these cells lack perilipin A, lipid droplets are coated with endogenous perilipin 2. When lipolysis was measured in control cells, the same rate of release of fatty acids was observed in both basal and stimulated conditions (Figure 8). Perilipin 2 is less effective than perilipin A at decreasing basal lipolysis and is not a substrate for PKA, so it does not

Figure 8. Perilipin A protects lipid droplets against basal lipolysis and increases PKA-stimulated lipolysis in NIH 3T3 CARΔ fibroblasts.

NIH 3T3 CARΔ fibroblasts were transduced to ectopically express perilipin A or β-galactosidase. At 44 hours post-transduction, cells were incubated with 600 μM ^{3}H-oleic acid for 4 hours to label the intracellular lipid pool. At the end of the 4-hour incubation, lipid loading medium was removed and cells were incubated with either basal medium (3% FAF BSA media containing 6 μM triacsin C and DMSO vehicle control) or stimulation medium (3% FAF BSA media containing 6 μM triacsin C, 10 μM forskolin and 0.5 mM IBMX) for 6 hours. Media samples were collected at 0, 2, 4 and 6 hours post-stimulation to assess fatty acid efflux. Data are expressed as the average nanomoles of fatty acids released per microgram of protein ± SEM of triplicate samples. Statistical analysis was done by 2-way analysis of variance (ANOVA). * $p < 0.05$ for perilipin A basal compared to perilipin A stimulated at the indicated time points.
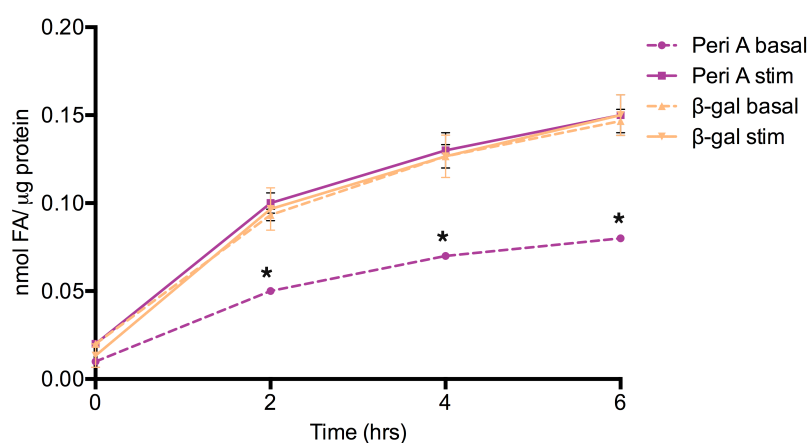
promote increased lipolysis in response to activated PKA (7,50). Consequently, lipolysis in cells expressing perilipin 2 is unaltered by intracellular cAMP levels.

Cells expressing wild-type perilipin A showed a 50% reduction in basal lipolysis compared to control cells expressing β-galactosidase (Figure 8). This finding supports previous observations that perilipin A serves a barrier function to reduce triacylglycerol turnover under basal conditions (7). Upon activation of PKA, a 2-fold increase in radiolabeled fatty acid release was observed in perilipin A-expressing cells relative to basal lipolysis. This release of fatty acids matched the maximal levels of lipolysis observed in cells expressing perilipin 2 under both basal and PKA-activated conditions. These results confirm previous observations that PKA-mediated phosphorylation of perilipin A facilitates lipolysis (17,40,50,85). Importantly, since these data recapitulate previous findings (Liang and Brasaemle, unpublished), they verify that our experimental conditions are working appropriately.

ATGL is not expressed in NIH 3T3 CARΔ fibroblasts. The endogenous lipases in NIH 3T3 CARΔ fibroblasts are currently unidentified. Therefore, since ATGL is widely expressed in cells and tissues (89,90,97), we asked if ATGL is one of the endogenous lipases expressed in our cell model. Semi-quantitative PCR revealed low levels of ATGL mRNA in NIH 3T3 CARΔ cells relative to very high levels of ATGL mRNA in 3T3-L1 adipocytes (not shown). However, we have never detected protein levels of ATGL on any of the many immunoblots of cell lysates of uninfected NIH 3T3 CARΔ fibroblasts.

To investigate ATGL expression in NIH 3T3 CARΔ cells in a more rigorous manner, immunoprecipitation analysis was performed. Immunoblotting of proteins immunoprecipitated from uninfected cell lysates containing 1 mg of total protein revealed

Figure 9. ATGL is not expressed in NIH 3T3 CARΔ fibroblasts

Immunoprecipitates of lysates of NIH 3T3 CARΔ fibroblasts revealed the absence of endogenous ATGL. For positive controls (ctrl), NIH 3T3 CARΔ cells were transduced with ATGL adenovirus for 24 hours prior to cell harvest. Cell lysates (1 mg of total protein) were immunoprecipitated with anti-ATGL antibody cross-linked to protein A-Sepharose beads. Rabbit pre-immune serum was used to precipitate proteins from cell lysates expressing ectopic ATGL as a negative control. For the input lane, 30 μg of total protein were loaded onto the gel. Data are representative of two experiments.
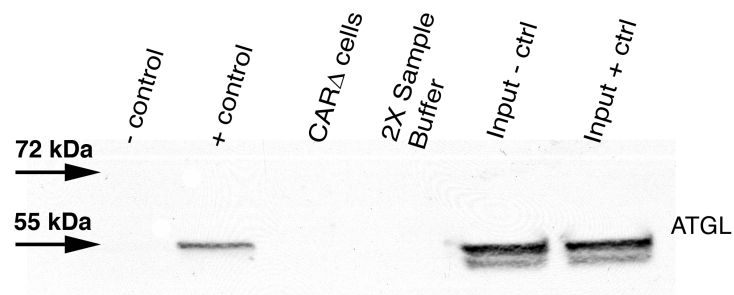
the absence of endogenous ATGL in NIH 3T3 CARΔ cells (Figure 9).

Choosing the adenoviral titer for ATGL expression. Previous work from our research group had shown that the phosphorylation of PKA site 5 of perilipin A is required for maximal lipolysis (Liang and Brasaemle, unpublished data). These experiments used NIH 3T3 CARΔ fibroblasts as the cell model; this cell line does not express endogenous perilipin A or HSL. In this study, we have shown that NIH 3T3 CARΔ cells also lack ATGL, a major lipase in adipocytes. Therefore, the next question we asked in this study was how the phosphorylation of serine 492 of perilipin A affects lipolysis catalyzed by ATGL.

Before beginning lipolysis studies, we first needed to determine the optimal adenoviral titer to use to drive ATGL expression. The ideal dose of adenovirus will promote the expression of sufficient ATGL to increase lipolysis when PKA is activated and perilipin becomes phosphorylated, but will not override the capacity of perilipin A to reduce lipolysis under basal conditions. To determine this viral titer, NIH 3T3 CARΔ cells were sequentially transduced with wild-type perilipin A adenovirus followed by increasing doses of ATGL adenovirus. Cells were lipid-loaded for the final 12 hours to stabilize perilipin and provide substrate for ATGL before harvesting the cells 2 days after the initial transduction. Total lipids were extracted from cells and the triacylglycerol content of the cells was quantified using an enzymatic assay (120).

As shown in Figure 10A, under basal conditions, cells expressing ectopic perilipin accumulated almost twice the amount of triacylglycerol in the absence of ATGL as that accumulated in uninfected cells. These results confirm previous findings that perilipin A facilitates triacylglycerol storage (7). In the absence of perilipin A, expression of

Figure 10. Titration of ATGL adenovirus in NIH 3T3 CARΔ fibroblasts

NIH 3T3 CARΔ fibroblasts were transduced with perilipin A adenovirus, ATGL adenovirus, or both perilipin A and ATGL adenoviruses. Uninfected cells were included as controls. Cells were incubated with 600 μM oleic acid for 12 hours prior to harvest at 48 hours post-transduction. Lipids were extracted from cells and triacylglycerol content was analyzed and expressed relative to total cell protein (A). Cell lysates were immunoblotted for perilipin A, ATGL and calnexin (B). Data are representative of two experiments each performed with duplicate samples.

(A)
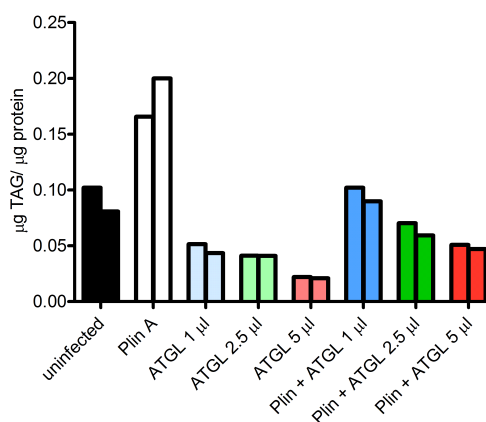
(B)
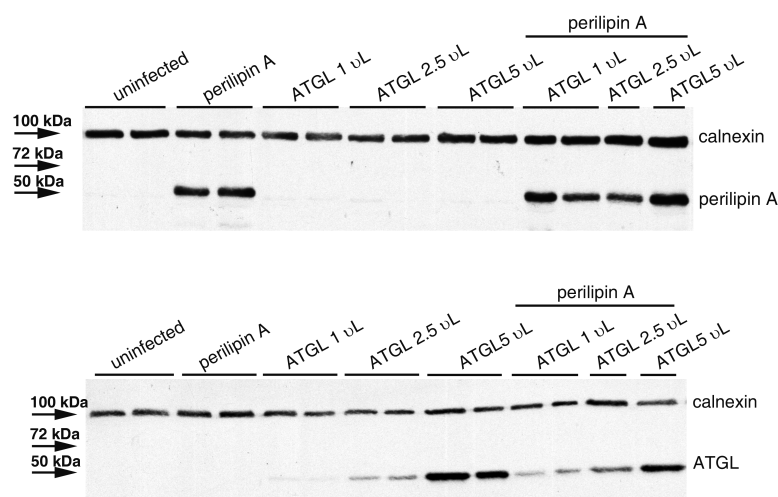
increasing levels of ATGL caused a dose-dependent decrease in the mass of triacylglycerol under basal conditions. At maximal levels of ATGL expression, the total triacylglycerol was approximately 25% the triacylglycerol of uninfected cells and approximately 12.5% the triacylglycerol of cells expressing perilipin A without ATGL. This reduction in triacylglycerol most likely results from the hydrolysis of triacylglycerol by ATGL when lipid droplets are minimally protected by perilipin 2. Importantly, ATGL activity was attenuated by the expression of perilipin A. Expression of perilipin A prior to the transduction of cells with a low dose of ATGL adenovirus restored the mass of triacylglycerol to that of uninfected cells. A dose-dependent decrease in triacylglycerol mass was observed with increasing levels of ATGL expression. Immunoblotting of cell lysates confirmed the expression of perilipin A and the dose-dependent expression of ATGL (Figure 10B). These results show that perilipin A can attenuate the decrease in triacylglycerol accumulation that accompanies ATGL expression. From these data, 1 μL of ATGL was shown to increase lipolysis without exceeding the capacity of perilipin A to reduce basal lipolysis. Subsequent lipolysis experiments were performed using this titer of ATGL adenovirus.

Basal lipolysis increases in the presence of ectopic ATGL in NIH 3T3 CARΔ fibroblasts. To initially address how the phosphorylation of perilipin A by PKA affects lipolysis catalyzed by ATGL, we performed a lipolysis experiment in NIH 3T3 CARΔ cells expressing wild-type perilipin A or the control protein β-galactosidase. ATGL was transduced into these cells 24 hours after transduction of the cells with perilipin A or β-galactosidase. Twenty-four hours after the second transduction, the cells were incubated for 4 hours with 600 μM ^{3}H-oleic acid complexed to FAF-BSA to radiolabel the pool of

stored triacylglycerols. Supplemental fatty acids were removed and cells were incubated with basal or stimulation medium. Lipolysis was estimated from the appearance of radiolabeled oleic acid in the media. Media samples were collected at 0, 2, 4 and 6 hours after stimulation and analyzed by liquid scintillation counting.

Lipolysis measurements in control cells expressing β-galactosidase, which have perilipin 2-coated lipid droplets, revealed similar rates of fatty acid release under both basal and stimulated conditions (Figure 11A). Similar results were obtained when lipolysis was measured in control cells in the absence of ATGL (Figure 8). Hence, these data confirm the inability of perilipin 2 to decrease basal lipolysis or facilitate stimulated lipolysis catalyzed by ATGL (19). In contrast, cells expressing perilipin A in the presence of ectopic ATGL showed a 40% reduction in the basal release of fatty acids when compared to stimulated lipolysis at 6 hours (Figure 11A). These results indicate that ectopic perilipin A reduces basal triacylglycerol turnover and increases stimulated lipolysis in NIH 3T3 CARΔ cells, even in the presence of ectopic ATGL.

Interestingly, the stimulated efflux of fatty acids from cells expressing ectopic perilipin A and ATGL was 1.8 times more than the maximal efflux of fatty acids measured in cells expressing endogenous perilipin 2 and ectopic ATGL (Figure 11A). Importantly, this was not observed in the absence of ATGL, where the stimulated release of fatty acids in cells expressing ectopic perilipin A matched the maximal levels of lipolysis observed in cells expressing endogenous perilipin 2 (Figure 8). Based on these findings, we hypothesized that the activity of ectopic ATGL increased basal lipolysis and thus reduced total triacylglycerol storage, particularly for perilipin 2-coated lipid droplets.

Figure 11. Ectopic expression of ATGL increases basal lipolysis in NIH 3T3 CARΔ fibroblasts

NIH 3T3 CARΔ fibroblasts were transduced to ectopically express wild-type perilipin A or β-galactosidase in combination with ATGL. Cells were incubated with 600 μM ^{3}H-oleic acid for 4 hours to label the intracellular lipid pool. At 48 hours post-transduction, lipid loading medium was removed and cells were incubated with either basal medium or stimulation medium for 6 hours. Media samples were collected at 0, 2, 4 and 6 hours post-stimulation to assess fatty acid efflux. Data are representative of 2 experiments and are expressed as the average nanomoles of fatty acids released per microgram of protein ± SEM of triplicate samples (A). Radiolabeled fatty acid incorporation into triacylglycerol and phospholipids was assessed by lipid extraction of cells harvested after the 4-hour labeling period and TLC analysis of lipids (B). Data for the incorporation of radiolabeled fatty acids into triacylglycerol and phospholipids are expressed as the average micrograms of oleic acid per 35 mm well ± SEM of duplicate samples. Total protein obtained from a 35 mm well was approximately 180 μg. Statistical analysis was done by 2-way ANOVA for the lipolysis data and 1-way ANOVA for TLC analysis. For lipolysis data,* $p < 0.05$ for β-gal basal, β-gal stimulated and perilipin A basal compared to perilipin A stimulated at the indicated time points. For triacylglycerol TLC data, subscripts (a,b) represent significant difference from each other with $p < 0.05$.

(A)
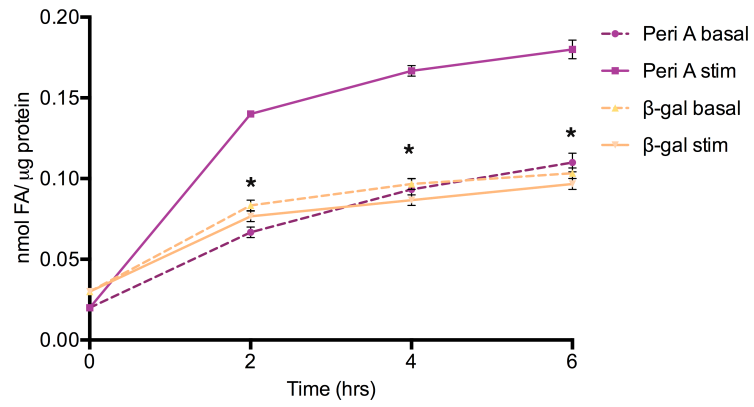
(B)
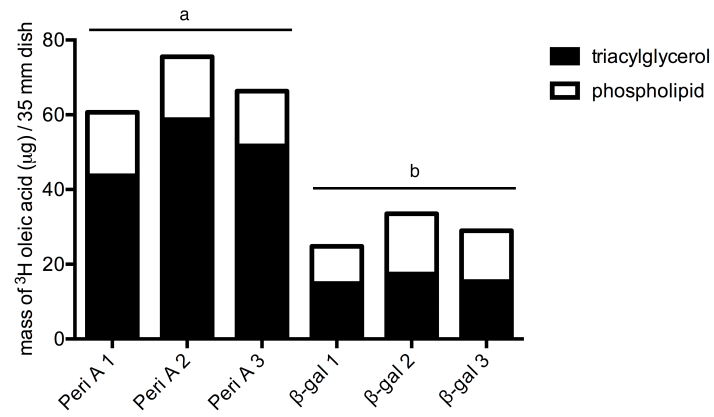
To test our hypothesis, we assessed cellular lipid content in this experiment by measuring the incorporation of radiolabeled oleic acid into triacylglycerol and phospholipids. If the ectopic expression of ATGL indeed affects basal lipolysis and reduces triacylglycerol storage, a larger percentage of the fatty acids supplemented to the cells during lipid loading would be directed to phospholipid synthesis rather than to triacylglycerol synthesis. Cells expressing perilipin A or β-galactosidase in the presence of ATGL were incubated with radiolabeled oleic acid for 4 hours to label intracellular lipids. At the end of the incubation period, supplemental lipids were removed and cells were harvested. Lipids from cell pellets were extracted and resolved by TLC. Bands corresponding to triacylglycerol and phospholipids were scraped and analyzed by liquid scintillation counting.

Lipid extractions and TLC analysis of cells expressing perilipin A revealed that the incorporation of radiolabeled fatty acids into triacylglycerols was 3 times higher than into phospholipids (Figure 11B). However, this ratio was reduced in control cells expressing perilipin 2; fatty acids were incorporated into phospholipids and triacylglycerols in an approximate 1:1 ratio. Importantly, cells expressing perilipin A incorporated 3.4 times more radiolabeled fatty acids into triacylglycerol than cells expressing perilipin 2. These data indicate that perilipin A-coated droplets store more triacylglycerols than perilipin 2-coated droplets in the presence of ATGL. The mechanism is likely through increased basal lipolysis in cells expressing perilipin 2, resulting in more rapid triacylglycerol turnover.

Phosphorylation of Ser492 of perilipin A is required for maximal PKA-stimulated lipolysis. We next addressed the question of how the phosphorylation of

serine 492 of perilipin A affects lipolysis catalyzed by ATGL. We expressed either wild-type perilipin or the variants perilipin S492A, perilipin Not5, or perilipin All6 in NIH 3T3 CARΔ cells using to the pre-established titers. ATGL was transduced into the cells 24 hours later. Twenty-four hours after the second transduction, the cells were incubated with 600 μM ^{3}H-oleic acid to radiolabel the pool of stored triacylglycerols. Supplemental fatty acids were removed after 4 hours and cells were incubated under basal or stimulated conditions as previously described. Media samples were collected during the next 6 hours to measure fatty acid efflux into the media as an estimate of lipolysis.

Under basal conditions, we observed comparable rates of basal lipolysis for 2 out of 3 tested variants; when compared to wild-type perilipin A, perilipin S492A and perilipin Not5 had similar rates of basal lipolysis (Figure 12A). This suggests that these variants are equally protective against basal triacylglycerol hydrolysis as unmodified perilipin A. The perilipin All6 variant showed a slight but significant decrease in basal fatty acid release at all time points. However, this decrease was not consistent among repetitions of experiments. Thus, we cannot conclude that the perilipin All6 variant was less protective against basal lipolysis than perilipin S492A or perilipin Not5. When PKA was activated to stimulate lipolysis, cells expressing the perilipin Not5 variant released similar levels of fatty acids when compared to cells expressing wild-type perilipin A (Figure 12B); cells expressing both wild-type perilipin A and perilipin Not5 released approximately 1.7-fold more fatty acids under stimulated conditions relative to basal conditions at 6 hours. Hence, these findings suggest that the phosphorylation of only serine 492 of perilipin A is sufficient to drive maximal stimulated lipolysis catalyzed by ATGL.

Figure 12. PKA-mediated phosphorylation of Ser 492 of perilipin A is required for maximal stimulated lipolysis in NIH 3T3 CARΔ cells ectopically expressing ATGL

NIH 3T3 CARΔ fibroblasts were transduced to ectopically express either perilipin A, or the perilipin variants S492A, All6, or Not5 in combination with ATGL. These cells were incubated with 600 μM ^{3}H-oleic acid for 4 hours to label intracellular lipids. At 48 hours post-transduction, lipid loading medium was removed and cells were incubated with either basal or stimulation medium for 6 hours. Media samples were collected at 0, 2, 4 and 6 hours post-stimulation to assess fatty acid efflux (A, B). The percent of fatty acids released was calculated based on the amount of fatty acids effluxed to the media at a given time point and the amount of radiolabeled oleic acid incorporated into triacylglycerol after the 4-hours lipid loading period. Protein levels of perilipin A and ATGL were confirmed by immunoblotting (C). Data are representative of 3 experiments and are expressed as the average percent of fatty acids released ± SEM of triplicate samples. Statistical analysis was done by 2-way ANOVA. * $p < 0.05$ for (A) All6 compared to perilipin A, (B) S492A and All6 compared to perilipin A at the indicated time points.
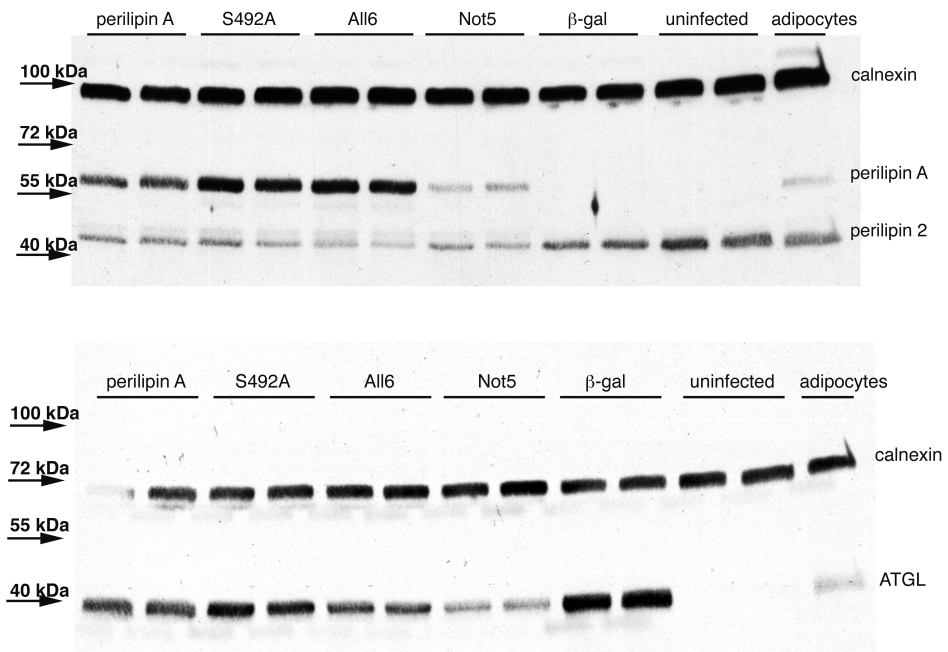
(A)
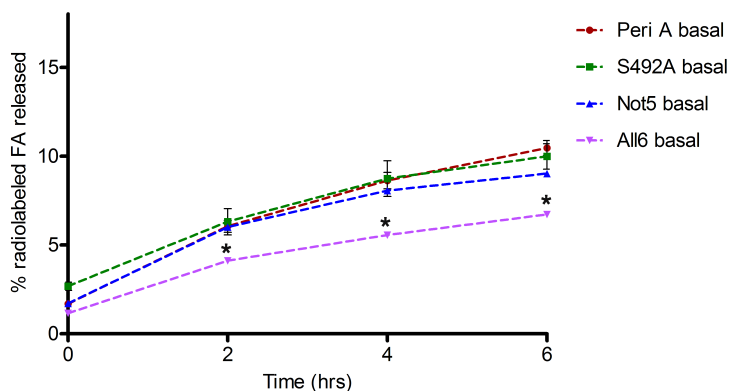
(B)
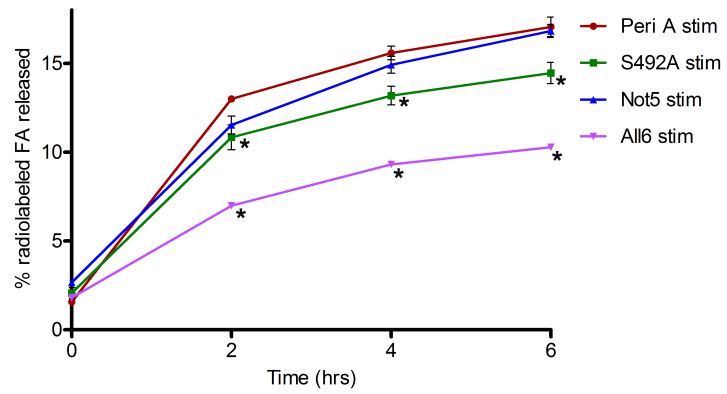
(C)

Perilipin S492A and perilipin All6 were significantly less effective at facilitating stimulated fatty acid release (Figure 12B). The mutation of serine 492 caused a 15% reduction in stimulated lipolysis relative to cells expressing wild-type perilipin A; this suggests that in the absence of PKA site 5, the phosphorylation of other PKA sites in perilipin A can facilitate lipolysis although not to maximal levels. Under stimulated conditions, cells expressing perilipin All6 showed a 1.5 fold increase in fatty acid release when compared to basal lipolysis for perilipin All6-expressing cells at 6 hours. However, this increase in the release of fatty acids did not exceed basal lipolysis levels in cells expressing wild-type perilipin A. This small increase in lipolysis could have been aided by the glutamic acid substitution in position 517. More importantly, these results indicate that phosphorylation of perilipin A is required for maximal mobilization of fatty acids from lipid droplets.

Lipid extraction of cells and TLC analysis of lipids were performed for cells expressing the different PKA site variants in one of the three experiments to assess the incorporation of fatty acids into triacylglycerol and phospholipids. Data from this experiment revealed that the majority of the radiolabeled fatty acids were incorporated into triacylglycerol rather than phospholipids (data not shown). This suggests that cells utilized the supplemented fatty acids mostly for triacylglycerol synthesis and storage, independently of the perilipin variant expressed. The mass of fatty acids incorporated into triacylglycerol was also similar among cells expressing different perilipin PKA site variants, with the exception of reduced incorporation of fatty acids into triacylglycerol in cells expressing perilipin All6. These results indicate that the perilipin PKA site variants have similar capacity to promote basal triacylglycerol storage in the presence of ectopic

ATGL.

Immunoblotting of cellular proteins confirmed the expression of the perilipin A variants and ATGL (Figure 12C). As expected, protein levels of endogenous perilipin 2 were higher in uninfected cells and cells expressing β-galactosidase when compared to cells expressing the perilipin PKA site variants. These results indicate that the perilipin variants were able to replace perilipin 2 on lipid droplets. Protein levels of the perilipin variants were similar to each other, except for the perilipin Not5 variant. Protein levels of ATGL were similar across all the samples except for cells expressing perilipin Not5. While conducting the experiments, we noticed some cytotoxicity in these cells, which could help to explain the reduced protein expression. Nonetheless, reduced expression of perilipin Not5 and ATGL in these cells did not appear to significantly affect the lipolysis data.

Together, these data suggest that phosphorylation of perilipin A serine 492 is needed for maximal lipolysis when ATGL is expressed. When Ser492 is mutated, phosphorylation of other PKA sites in perilipin A can facilitate lipolysis, although not to maximal levels. Importantly, these experiments measured lipolysis in cells expressing ATGL in the absence of CGI-58, which is not endogenously expressed in this cell model (Sahu and Brasaemle, unpublished). Therefore, the phosphorylation of perilipin A serine 492 can facilitate ATGL-mediated lipolysis independently of the expression of CGI-58.

Increasing expression of CGI-58 increases basal lipolysis in NIH 3T3 CARΔ cells ectopically expressing perilipin A and ATGL. The regulation of ATGL activity largely depends on its interactions with its co-activator, CGI-58, and the phosphorylation status of perilipin A. Under basal conditions, CGI-58 binds to unphosphorylated perilipin

A on lipid droplets (9). Phosphorylation of perilipin A by PKA releases CGI-58 into the cytosol where it can interact and co-activate ATGL. A previous study suggested that the phosphorylation of PKA sites 5 and 6 of perilipin A is required for the release of CGI-58 from perilipin A (10). For our next study, we assessed how the phosphorylation of perilipin A serine 492 affects ATGL-mediated lipolysis when CGI-58 is expressed. Prior to testing lipolysis, we first conducted an experiment to identify a titer of CGI-58 adenovirus that would yield detectable amounts of CGI-58 protein and increase PKA-stimulated lipolysis. NIH 3T3 CARΔ cells were first transduced with a fixed dose of perilipin A adenovirus and transduced one day later with both ATGL and CGI-58 adenoviruses. A single dose of ATGL adenovirus was selected with increasing titer of CGI-58 adenovirus. Cells were lipid loaded with 600 μM ^{3}H-oleic acid for 4 hours prior to incubation with basal or stimulation media. Media samples were collected at 0, 2, 4 and 6 hours post-stimulation to assess fatty acid efflux.

During the first 2 hours of basal conditions, we observed no differences in the efflux of fatty acids into the culture medium among cells treated with the different CGI-58 doses (Figure 13A). However, at 4 and 6 hours, cells expressing lower levels of CGI-58 released 17% more fatty acids than cells expressing higher amounts of CGI-58 when the mass of fatty acids was calculated relative to total cell protein. A similar pattern was observed in response to the stimulation of lipolysis; cells expressing lower CGI-58 released the highest mass of fatty acids when calculated relative to cell protein (Figure 13B). We also noticed less difference between the relative rates for basal and stimulated lipolysis as the level of CGI-58 expression increased. For example, in cells transduced with 4 μL of CGI-58 adenovirus, stimulated release of fatty acids was only 6% higher

Figure 13. Increased expression of CGI-58 in NIH 3T3 CARΔ cells with ectopic perilipin A and ATGL increases basal lipolysis and impairs lipid storage

NIH 3T3 CARΔ fibroblasts were transduced with adenoviruses to drive the expression of wild-type perilipin A, ATGL and increasing doses of CGI-58. Uninfected cells and cells expressing ectopic β-galactosidase, ATGL and a low titer dose of CGI-58 were included as controls. Cells were incubated with 600 μM ^{3}H-oleic acid for 4 hours. At 48 hours post-transduction, lipid loading medium was removed and cells were incubated with either basal or stimulation medium for 6 hours. Media samples were collected at 0, 2, 4 and 6 hours post-stimulation to assess fatty acid efflux (A, B). Data are representative of 2 experiments and are expressed as the average nanomoles of fatty acids released per microgram of protein ± SEM of triplicate samples (A, B), or as the average percent of fatty acids released ± SEM of triplicate samples (D, E). Radiolabeled fatty acid incorporation into triacylglycerol and phospholipids was assessed by lipid extraction of cells harvested after the 4 hour labeling period and TLC analysis of lipids (C). Data from TLC analysis are expressed as the average micrograms of oleic acid per 35 mm well ± SEM of duplicate samples (C). Total protein obtained from a 35-mm well was approximately 240 μg. Immunoblotting was performed to confirm expression of the different proteins (F). Statistical analysis was done by 2-way ANOVA for the lipolysis data and 1-way ANOVA for TLC analysis. For lipolysis data, * $p < 0.05$ for (A) CGI-58 0.5 and 1 μL compared to CGI-58 4 μL, and (B, D, E) CGI-58 0.5, 1 and 2 μL compared to CGI-58 4 μL at the indicated time points. For triacylglycerol data in (C), subscripts (a,b,c) represent significant differences from each other at $p < 0.05$. Samples with the same subscript are not different from each other.
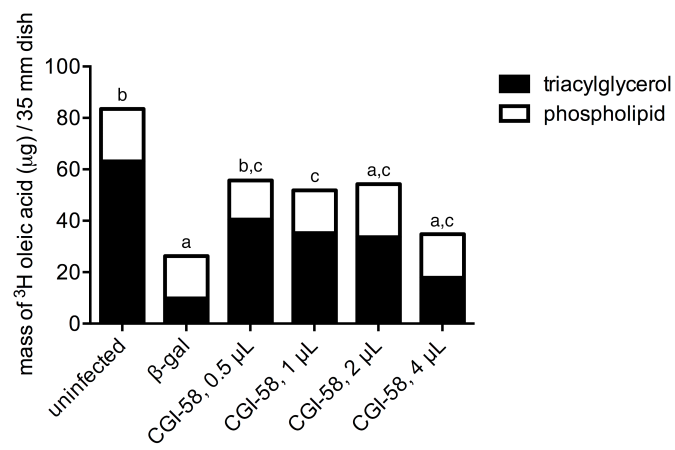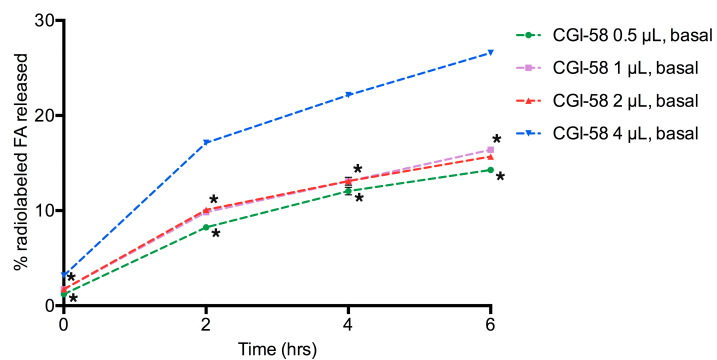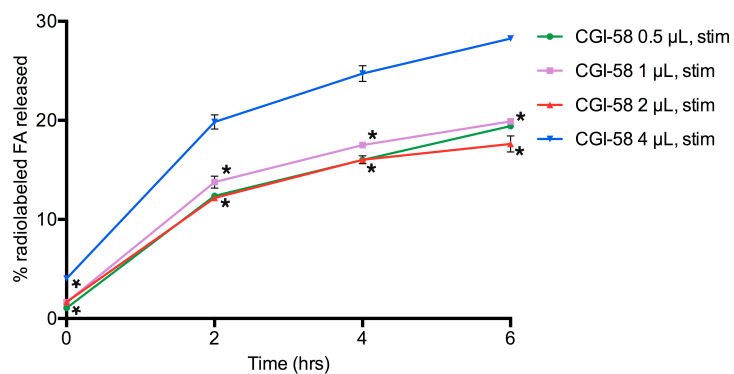
(A)
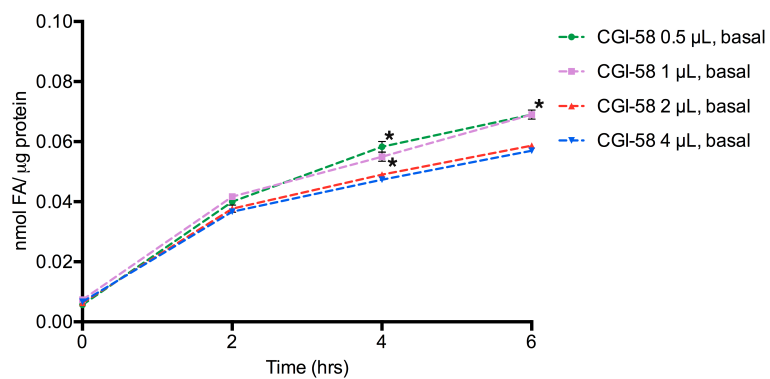
(B)
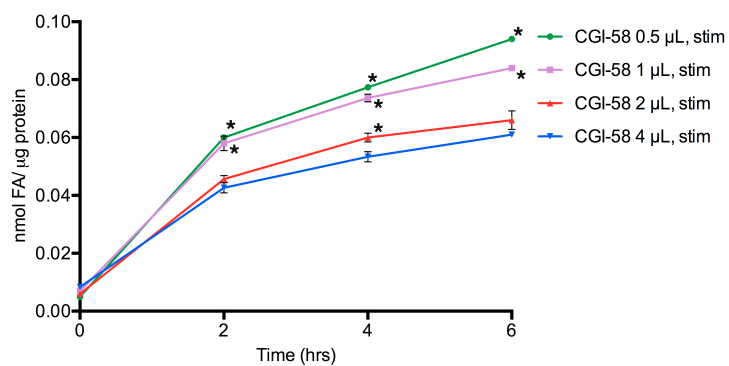
(C)

(D)

(E)

(F)
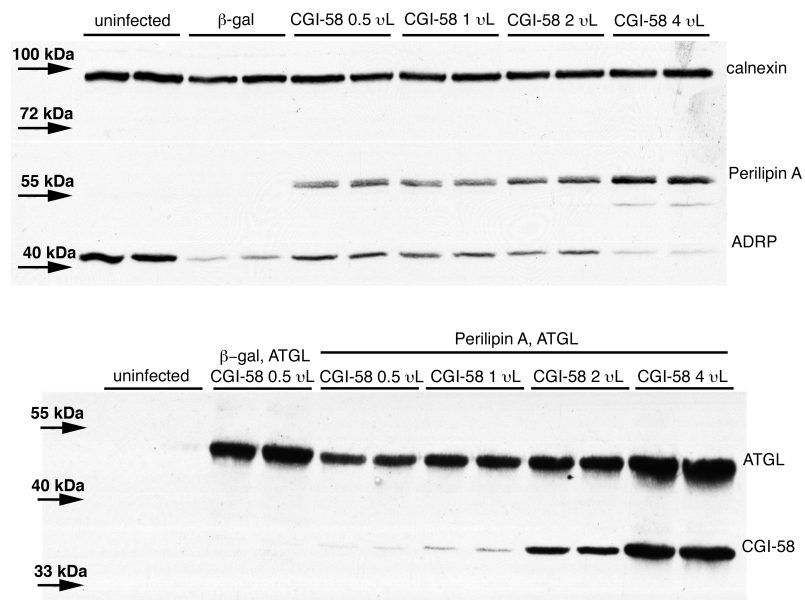
than that in basal conditions at 6 hours. In contrast, cells transduced with 0.5 μL of CGI-58 adenovirus had 19% higher release of fatty acids following stimulation of lipolysis when compared to the basal release of fatty acids at 6 hours. Control cells expressing β-galactosidase, ATGL and CGI-58 had equal rates of basal and stimulated lipolysis, but also had the lowest release of fatty acid mass when compared to cells expressing perilipin A, ATGL and doses of CGI-58 (data not shown).

These findings were the opposite of what might be expected; higher expression of CGI-58 yielded lower release of fatty acids. To investigate the cause, we extracted lipids from cells collected immediately following lipid loading incubations. As shown in Figure 13C, lipid extraction and TLC analysis of cells expressing perilipin A, ATGL and CGI-58 revealed that the incorporation of fatty acids into triacylglycerol decreased in cells with higher levels of CGI-58. Thus, these data suggest that higher levels of CGI-58 impair triacylglycerol storage in these cells.

Since the total incorporation of fatty acids into triacylglycerol varied with protein levels of CGI-58 (Figure 13C), we re-arranged the data to express them as the percentage of fatty acids released relative to the initial mass of fatty acids incorporated into triacylglycerol. When expressed relative to total triacylglycerol, the overall order of the lipolysis curves reversed. Data in Figure 13C and 13D show that cells expressing the highest protein mass of CGI-58 (from 4 μL of adenovirus) released a higher percentage of fatty acids than cells expressing lower levels of CGI-58 (from 2, 1, 0.5 μL of adenovirus) under both basal and stimulated conditions.

Taken together, these data suggest that increased expression of ectopic CGI-58 in NIH 3T3 CARΔ cells also expressing ectopic perilipin A and ATGL increases basal

triacylglycerol turnover. Furthermore, data suggest that protein levels of perilipin A are limiting in this cell model, so it is possible that excess CGI-58 in the cells is not bound to perilipin A under basal conditions and hence, is available to activate ATGL. The hydrolytic activity of ATGL then increases basal lipolysis, resulting in higher turnover of triacylglycerol during incubation of cells with radiolabeled oleic acid. Most importantly, our findings suggest that the protein ratio of CGI-58 to perilipin A is critical for measurements of perilipin A-mediated control of both basal and stimulated lipolysis. Based on these findings, 0.5 μL of CGI-58 adenovirus were chosen for subsequent experiments. This was the minimal tested titer that increased stimulated lipolysis and least affected basal triacylglycerol turnover.

Lastly, immunoblotting of cell lysates from cells expressing perilipin A, ATGL and CGI-58 confirmed comparable protein levels of perilipin A between samples and the dose-responsive expression of CGI-58 (Figure 13E). We also noticed an increase in protein levels of ATGL with increased expression of CGI-58. These data suggest that CGI-58 may increase the protein stability of ATGL; however, more experiments are needed to examine this relationship further.

Phosphorylation of Ser492 of perilipin A promotes maximal PKA-stimulated lipolysis in NIH 3T3 CARΔ cells ectopically expressing perilipin, ATGL and CGI-58. We have shown that the phosphorylation of serine 492 of perilipin A is critical for PKA-stimulated lipolysis in both the presence and absence of ATGL. However, NIH 3T3 CARΔ cells do not express CGI-58, the co-activator of ATGL. For the final experiment, we wanted to investigate how the phosphorylation of perilipin A serine 492 affects lipolysis in the presence of ectopic CGI-58. To address this question, we examined basal

Figure 14. PKA-mediated phosphorylation of Ser 492 of perilipin A contributes to maximal stimulated lipolysis in NIH 3T3 CARΔ cells ectopically expressing ATGL and CGI-58

NIH 3T3 CARΔ fibroblasts were transduced to ectopically express either (A, B) perilipin A or β-galactosidase in combination with ATGL and CGI-58 or (B-D) perilipin A, or the perilipin variants S492A, All6, or Not5 in combination with ATGL and CGI-58. Cells were incubated with 600 μM ^{3}H-oleic acid for 4 hours to radiolabel intracellular lipids. Fatty acids were then removed and the cells were incubated with either basal or stimulation medium for 6 hours. Media samples were collected at 0, 2, 4 and 6 hours to assess fatty acid efflux (A, C-D). Data are representative of 2 experiments and are expressed as the average percent fatty released ± SEM of triplicate samples (A, C-D). Radiolabeled fatty acid incorporation into triacylglycerol and phospholipids was assessed by lipid extraction of cells harvested after the 4 hour labeling period and TLC analysis of lipids (B). Data from TLC analysis are expressed as the average micrograms of oleic acid per 35-mm well ± SEM of duplicate samples (B). Total protein obtained from a 35 mm well was approximately 180 μg. Protein expression was confirmed by immunoblotting (E). Statistical analysis was done by 2-way ANOVA for the lipolysis data and 1-way ANOVA for TLC analysis. For lipolysis data, * $p < 0.05$ for (A) β-gal basal, β-gal stimulated and perilipin A basal compared to perilipin A stimulated; (C) S492A and All6 compared to perilipin A; (D) All 6 compared to perilipin A at the indicated time points. For triacylglycerol data in (B), subscripts (a,b,c,d) represent significant difference from each other with $p < 0.05$. Samples with the same subscript are not different from each other.

(A)
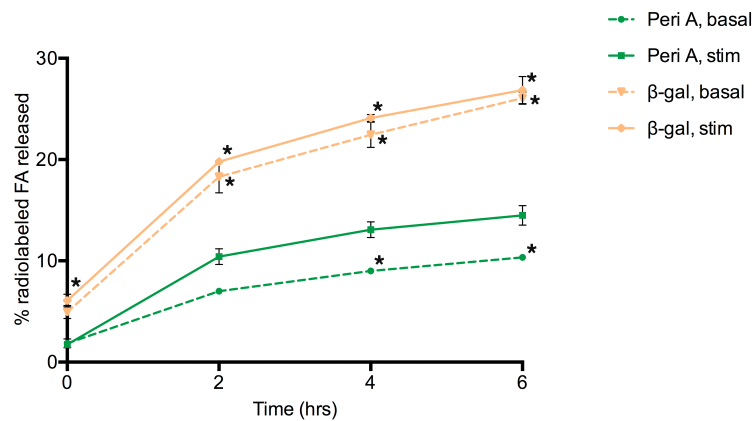
(B)
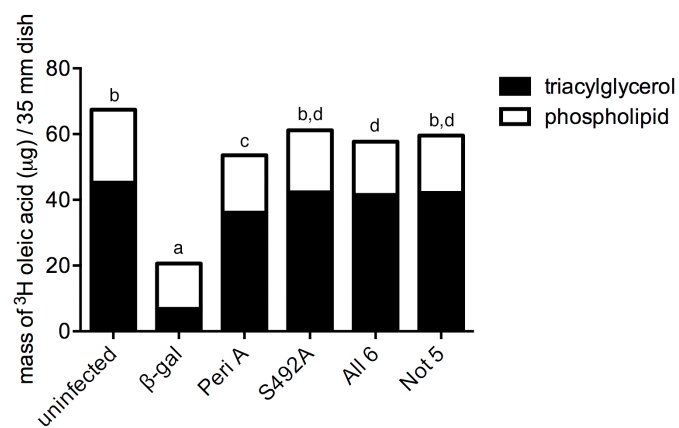
(C)
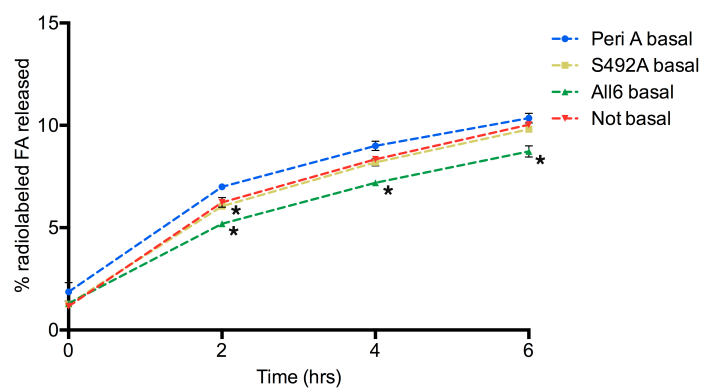
(D)
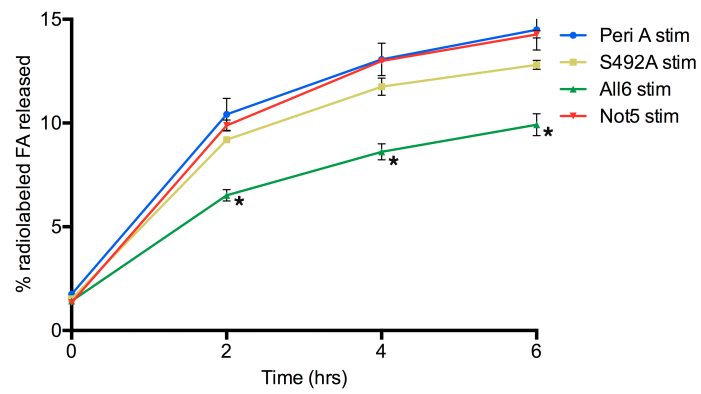
(E)

and stimulated lipolysis in NIH 3T3 CARΔ cells expressing the perilipin PKA site variants, ATGL and CGI-58. NIH 3T3 CARΔ cells were first transduced with the different perilipin variants, followed by co-transduction with ATGL and CGI-58 adenoviruses 24 hours later. Cells were lipid loaded with 600 μM ^{3}H-oleic acid for 4 hours followed by incubation with basal or stimulation media. Media samples were collected at 0, 2, 4 and 6 hours post-stimulation to assess the appearance of radiolabeled fatty acids in the media.

Control cells transduced with β-galactosidase adenovirus had equal rates of basal and stimulated lipolysis in the presence of ectopic ATGL and CGI-58 (Figure 14A). Thus, the expression of CGI-58 with ATGL does not alter lipolysis when perilipin 2 coats lipid droplets; these results were similar to data obtained for cells expressing β-galactosidase and ATGL (Figure 11A) and β-galactosidase when only endogenous lipases are present (Figure 8). The incorporation of fatty acids into triacylglycerol in β-galactosidase-expressing control cells was approximately 20% the amount of fatty acids incorporated into triacylglycerol in cells expressing perilipin A (Figure 14B). Higher fatty acid incorporation into triacylglycerol in perilipin A-expressing cells verifies that perilipin A is protective of newly synthesized triacylglycerol under basal conditions even in the presence of ectopic CGI-58.

Cells expressing wild-type perilipin A in the presence of ATGL and CGI-58 showed decreased release of fatty acids under basal conditions when compared to stimulated lipolysis. However, the reduction in basal lipolysis relative to stimulated lipolysis was only 29% in cells co-expressing perilipin A, CGI-58 and ATGL compared to a 40% reduction in cells co-expressing perilipin A and ATGL. The reduced difference

between the rates of basal and stimulated lipolysis in these experiments suggests that the expression of CGI-58 increases basal lipolysis in cells expressing perilipin A and ATGL when compared to cells expressing ATGL without CGI-58.

Finally, we tested how the perilipin PKA site variants mediate lipolysis in the presence of ATGL and CGI-58. We found no major differences in the basal lipolysis of cells expressing perilipin S492A or perilipin Not5 compared to cells expressing wild-type perilipin A at 4 and 6 hours after removal of supplemental fatty acids (Figure 14C). Cells expressing the perilipin All6 variant showed a slight but significant reduction in basal fatty acid release compared to cells expressing wild-type perilipin A. Under conditions of stimulated lipolysis, cells expressing the perilipin Not5 variant released similar levels of fatty acids to cells expressing wild-type perilipin A (Figure 13D), suggesting that the phosphorylation of serine 492 of perilipin A alone promotes maximal PKA-stimulated lipolysis in NIH 3T3 CARΔ cells ectopically expressing ATGL and CGI-58. Cells expressing perilipin S492A released 12% lower levels of fatty acids when compared to cells expressing wild-type perilipin A at 6 hours after the addition of forskolin and IBMX; however, these findings were not statistically significant. Cells expressing the perilipin All6 variant released 30% lower levels of fatty acids in the presence of ATGL and CGI-58 at 6 hours; these results were statistically significant. These data suggest that phosphorylation of perilipin A is necessary for PKA-mediated lipolysis and that the phosphorylation of Ser492 alone is sufficient for maximal stimulated lipolysis in cells expressing ectopic ATGL and CGI-58.

Immunoblotting of cell lysates confirmed comparable levels of expression of the perilipin A PKA site variants, as well as the expression of ectopic ATGL and CGI-58

(Figure 14E). Lipid extraction and TLC analysis of cells expressing the perilipin variants, ATGL and CGI-58 revealed no differences in the mass of radiolabeled fatty acids incorporated into triacylglycerols in cells expressing perilipin S492A, perilipin Not5 and perilipin All6. Data shown in Figure 14B indicate a small but significant decrease in the incorporation of fatty acids into triacylglycerol in cells expressing wild-type perilipin A when compared to the other perilipin variants, but these differences are likely due to experimental variability rather than functional differences.

DISCUSSION

The storage and mobilization of triacylglycerols from adipose reserves is a tightly regulated process. Perilipin A embedded in lipid droplets is important for these control mechanisms. In fed conditions, or basal state, perilipin A decreases basal lipolysis by at least two mechanisms. First, perilipin A acts as barrier and shields the lipid droplet core from cytosolic lipases (7). Second, perilipin A binds CGI-58 and prevents it from activating ATGL (9,10). Perilipin A also controls lipolysis under stimulated conditions, when the body has higher demand for stored energy. Activation of lipolysis through the signaling of β-adrenergic receptors increases intracellular cAMP levels, which leads to the activation of PKA. Phosphorylation of perilipin A by PKA promotes lipolysis by facilitating the docking of phosphorylated HSL on lipid droplets and by releasing CGI-58 into the cytosol (9,16). Free CGI-58 co-activates ATGL, which can then initiate lipolysis by hydrolyzing triacylglycerols (97). Although the perilipin A-mediated sequestration and release of CGI-58 from the lipid droplet has been proposed to be a major control point in the regulation of adipocyte lipolysis, it is likely that the phosphorylation of perilipin A facilitates lipolysis through additional mechanisms. In this study, we aimed to gain further understanding of how the phosphorylation of perilipin A, specifically phosphorylation of serine 492 in the carboxyl terminus of perilipin A, enables PKA-stimulated lipolysis.

The major finding of this study is that the phosphorylation of serine 492 of perilipin A is critical for maximal activation of lipolysis by ATGL. Here we show that in cells ectopically expressing ATGL, expression of a perilipin variant in which only serine 492 was available to be phosphorylated facilitated maximal stimulated lipolysis upon

activation of PKA. Moreover, phosphorylation of serine 492 facilitated maximal

stimulated lipolysis in cells expressing both ectopic ATGL and CGI-58. Additionally, we

observed that in the absence of PKA site 5, the phosphorylation of serine residues within

PKA sites 1-4 and 6 can drive significant PKA-stimulated lipolysis catalyzed by ATGL.

These findings are consistent with previous literature indicating that phosphorylation of

both PKA site 5 and PKA site 6 of perilipin A facilitates lipolysis by releasing CGI-58

from perilipin A to co-activate ATGL (10). Hence, one mechanism by which the

phosphorylation of serine 492 can increase lipolysis in NIH 3T3 CARΔ cells is by

facilitating the release of CGI-58 from perilipin A for subsequent co-activation of ATGL.

Earlier studies from our group have shown that under stimulated conditions,

phosphorylation of serine 492 of perilipin A alone promotes 78% of the maximal

lipolysis catalyzed by endogenous lipases in NIH 3T3 CARΔ cells expressing wild type

perilipin A (Liang and Brasaemle, unpublished). Endogenous lipases in these cells have

not been identified. HSL, a major adipocyte lipase, is absent from NIH 3T3 CARΔ cells.

In this study, we use immunoprecipitations to show that ATGL is not endogenously

expressed the cells. CGI-58, the co-factor for ATGL, is also absent in these cells (Sahu

and Brasaemle, unpublished). Yet, ectopically expressed ATGL had significant

hydrolytic activity in NIH 3T3 CARΔ cells; basal lipolysis in cells expressing

endogenous perilipin 2 (β-galactosidase control) or ectopic perilipin A increased with the

expression of ectopic ATGL, even in the absence of ectopic CGI-58. Therefore, another

major finding of the current study is that, in addition to the previously characterized

release of CGI-58 (10), the phosphorylation of serine 492 of perilipin A facilitates

lipolysis through a general mechanism independent of the availability of CGI-58 to

activate ATGL. This mechanism promotes lipolysis catalyzed by ATGL, and other endogenous lipases in NIH 3T3 CARΔ cells.

If the activation of ATGL-mediated lipolysis by perilipin A is not limited by the availability of CGI-58, then the phosphorylation of perilipin A serine 492 could facilitate lipolysis by at least two possible mechanisms. First, the phosphorylation of serine 492 could induce a conformational change in the carboxyl terminus of perilipin A to expose new binding sites for lipases on the phospholipid monolayer of lipid droplets. Work by Yang and co-workers shows that, following stimulation of lipolysis, increased recruitment of ATGL to lipid droplets is observed only in cells that express perilipin A (99). However, it is important to mention that studies have shown that perilipin A and ATGL probably do not directly interact; perilipin 5 is the only perilipin that has been shown to directly bind ATGL (19,69). Thus, an alternative mechanism could be that the phosphorylation of serine 492 alters the conformation of perilipin A to reveal binding sites on perilipin for other proteins that help to modulate ATGL activity. An example of such a protein could be G0/G1 switch gene 2, or G0S2.

G0S2 is highly expressed in adipose tissue and differentiated adipocytes (99). Recent studies have identified G0S2 as a negative regulator of ATGL's triacylglycerol hydrolase activity (99). G0S2 binds directly to ATGL and inhibits its lipase activity, even in the presence of CGI-58 (98). Hence, the binding of G0S2 to ATGL is probably not competitive with CGI-58, the co-activator of ATGL. Furthermore, G0S2 has been shown to localize primarily to the cytoplasm of cultured adipocytes with low levels on the surfaces of lipid droplets under basal conditions; isoproterenol treatment significantly increases recruitment of a complex of G0S2 with ATGL to lipid droplets. Based on these

findings, we can speculate that the phosphorylation of perilipin A by PKA could affect the binding or conformation of G0S2 on lipid droplets. Perilipin-mediated alterations in G0S2 could, in turn, facilitate the access of ATGL to triacylglycerols within lipid droplets for the catalysis of lipolysis.

Our findings suggest that, in the absence of perilipin PKA site 5, phosphorylation of PKA sites 1-4 and 6 may be sufficient for the activation of maximal lipolysis in cells expressing ectopic ATGL and CGI-58, but not when ATGL is expressed in the absence of CGI-58. Although stimulated lipolysis in cells expressing perilipin S492A was not significantly different than that of cells with wild-type perilipin A, there was a trend towards reduced lipolysis when both CGI-58 and ATGL were expressed. Because previous literature (42) and the present study indicate that phosphorylation of serine 492 of perilipin A is required for maximal lipolysis, we expected perilipin S492A to be significantly less effective than perilipin Not5 at facilitating lipolysis in the presence of ATGL and CGI-58. It is possible that conducting longer measurements or analyzing data collected from additional experimental repetitions will reveal that the trend towards a decrease in stimulated lipolysis is significant.

Another unexpected finding is that the addition of CGI-58 to the cells did not increase stimulated lipolysis compared to cells expressing ATGL only; similar levels of stimulated lipolysis were observed in the presence and absence of CGI-58. These findings differ from *in vitro* studies in which addition of CGI-58 to cell extracts containing ATGL increased triacylglycerol hydrolase activity by up to 20-fold when compared to extracts containing ATGL alone (97). The modest effect of CGI-58 observed in the present study is likely due to mechanisms specific to intact cells that are

not observed when testing lysed cell extracts for triacylglycerol hydrolase activity; these mechanisms likely fine-tune lipolysis to prevent excessive activation of ATGL by CGI-58.

In this study, the relative contribution of the phosphorylation of PKA site 6 (serine 517) to the activation of PKA-stimulated lipolysis is not fully clear. Because perilipin with an alanine substitution for serine 517 is difficult to express in cells (112), the perilipin variants Not5 and All6 used in this study included a glutamic acid substitution in PKA site 6. Glutamic acid was previously shown to be a permissible substitution for serine 517 (112). Recent work from our group suggests that polar or charged residues are required at the carboxyl terminus of perilipin A to target the nascent protein to lipid droplets (Daley and Brasaemle, unpublished). Additionally, perilipin variants with alanine substitutions for serine in position 517 followed by a negatively charged FLAG epitope tag localized to lipid droplets (42), supporting a need for polar or charged residues at the carboxyl terminus. Lipolysis experiments in cells expressing these FLAG-tagged perilipin variants showed that serine 517 in PKA site 6 is essential for the regulation of ATGL-mediated lipolysis (42); however, those findings are likely to be affected by the overall negative charge of the FLAG tag. In the current study, the negatively charged glutamate is likely sufficient to maintain the polar nature of the carboxyl terminus of perilipin A, allowing the protein to localize to lipid droplets. However, a potential complication of having glutamic acid in position 517 is that it is a phosphomimetic residue. Phosphates and carboxylates are both acidic, but they differ in size, number of oxygens, and number of negative charges at neutral pH (123). Yet, there are reports in the literature where aspartic acid or glutamic acid substitution of

phosphoserine residues can partially or completely mimic the effects of phosphorylation

(123). If the phosphorylation of PKA site 6 of perilipin A participates in the activation of

lipolysis, the mimetic effect of glutamic acid could increase lipolysis under basal and

stimulated conditions. To fully investigate the role of perilipin PKA site 6 in PKA-

stimulated lipolysis without the use of phosphomimetic mutations or epitope tags, it is

necessary to identify a non-charged or positively charged amino acid that can be

substituted for serine in position 517 to allow the targeting of perilipin A to lipid droplets.

The presence of a negatively charged glutamic acid residue in PKA site 6 may

explain our findings regarding the mutated variant of perilipin A in which all of the serine

residues within PKA sites have been mutated to alanine or glutamic acid (perilipin All6).

We found that perilipin All6 was the least effective variant at facilitating ATGL-mediated

lipolysis in response to forskolin and IBMX. Yet, this variant was able to facilitate a 1.5-

fold increase in stimulated fatty acid release relative to the basal state 6 hours after

activation of lipolysis in cells expressing ectopic ATGL. Notably, this increase was only

1.2-fold in previous experiments conducted in the absence of ATGL when only

endogenous lipases were present (Liang and Brasaemle, unpublished). Studies by

Granneman and coworkers indicate that the phosphorylation of PKA site 5 and 6 of

perilipin A mediates the release of CGI-58 from lipid droplets to allow its interaction

with ATGL (10). Hence, the glutamic acid substitution in PKA site 6 could potentially

mimic the effect of phosphorylation, consequently activating lipolysis in cells expressing

ectopic ATGL. Another possible explanation for the increased lipolysis observed in cells

expressing perilipin All6 and ATGL is the phosphorylation of additional sites in perilipin

A. Phosphoproteomics studies using mouse fat tissues have identified multiple other

phosphorylation sites in perilipin A in addition to the 6 PKA consensus sites previously identified (124-126). All of the additional sites remained intact in the All6 variant; thus, it is possible that phosphorylation of additional sites contributes to partial activation of ATGL-mediated lipolysis through as yet uncharacterized mechanisms.

An additional finding of the current study is that determining the correct protein level of CGI-58 relative to perilipin A is critical to obtaining physiologically relevant regulation of lipolysis in this model system. Cells expressing endogenous perilipin 2, ectopic ATGL and CGI-58 incorporated only 30% of radiolabeled fatty acids into triacylglycerol relative to cells expressing perilipin A, ATGL and CGI-58. This decrease in triacylglycerol storage in perilipin 2-expressing cells is likely due to increased activation of ATGL by CGI-58 in the cells, which, in turn, increases basal lipolysis. Furthermore, our results showed that, in cells expressing perilipin A and ATGL, as the expression of CGI-58 increased, the amount of fatty acids released in response to PKA stimulation decreased, contrary to expectations. The major cause was a dose-dependent reduction in the incorporation of fatty acids into triacylglycerols during the lipid loading period with increased levels of CGI-58. Thus, it was important to express the data as the mass of fatty acid released relative to the total mass of fatty acid incorporated into triacylglycerol during lipid loading. Expressing the data this way revealed that cells with the highest protein levels of CGI-58 released a higher percentage of fatty acids than cells expressing lower levels of CGI-58 under both basal and stimulated conditions. From these data, and consistent with the current model for the regulation of lipolysis, we conclude that excessive CGI-58 that cannot be sequestered by perilipin A is free to activate ATGL, increasing lipolysis even during the lipid loading period. Thus, it was

important for our studies to adjust the relative expression of CGI-58 relative to perilipin A to ensure the sequestration of CGI-58 and adequate control of basal lipolysis.

Studies in the literature provide further evidence that the sequestration of CGI-58 by perilipin A is critical to maintain lipid homeostasis. In humans, two heterozygous frameshift mutations (p.Leu-404fs, p.Val-398fs) of perilipin A have been associated with serious health complications such as lipodystrophy, insulin-resistant diabetes, hypertriglyceridemia and hepatic steatosis (127). These mutations induce the synthesis of a mutated variant of perilipin A with aberrant C-terminal amino acids. Bimolecular fluorescence complementation studies in 3T3-L1 preadipocytes expressing the mutated perilipin revealed that, unlike wild-type perilipin A, these perilipins fail to reduce the interaction between CGI-58 and ATGL (128). These results suggest that the mutated perilipins cannot sequester CGI-58 on lipid droplets under basal conditions, leading to increased basal lipolysis. Consequently, patients carrying these perilipin mutations have reduced triacylglycerol accumulation in adipocyte lipid droplets due to increased triacylglycerol turnover. Knockdown of either CGI-58 or ATGL in 3T3-L1 cells expressing the mutated perilipins significantly reduced basal lipolysis, indicating that the increase in basal lipolysis associated with the mutated perilipins is due to enhanced activation of ATGL by CGI-58. Thus, this study supports our conclusion that the sequestration of CGI-58 by perilipin A is critical to suppress ATGL activity in the basal state.

An interesting observation from experiments in which both ATGL and CGI-58 were expressed is that CGI-58 appears to stabilize ATGL. In these experiments, cells were transduced with constant doses of perilipin A and ATGL adenoviruses and

increasing doses of CGI-58 adenovirus. Protein levels of ATGL increased when higher

doses of CGI-58 adenovirus were used, suggesting increased stability. Protein levels of

perilipin A also increased with increasing expression of CGI-58; however, the increase in

perilipin A was less dramatic than the increase in ATGL. Because the immunoblots in

these experiments used lysates from cells in basal conditions, CGI-58 should have been

bound to the carboxyl terminus of perilipin A on lipid droplets. Thus, we speculate that

under basal conditions, CGI-58 forms a complex with perilipin A at the surfaces of lipid

droplets and with ATGL in either the cytoplasm or on lipid droplets. These associations

stabilize both proteins by extending the proteins' half-lives by preventing their

degradation.

During the process of optimizing the experimental conditions for the lipolysis

experiments, we found that shorter incubations of cells with fatty acids maximize the

expression of ectopic perilipin A while minimizing the expression of endogenous

perilipin 2. Because adenoviral expression vectors drive limited expression of proteins,

optimal lipid loading conditions to stabilize perilipin A should be empirically determined

for a given experiment. This is a particularly important consideration in the design of

experiments addressing the function of perilipin A in cells that express endogenous

perilipin 2. Perilipin 2 cannot reduce basal lipolysis as well as perilipin A and does not

respond to the activation of PKA (39,50); hence, it is important to minimize the

population of cells expressing perilipin 2 for these studies.

In conclusion, this study shows that the phosphorylation of serine 492 of perilipin

A is required to drive maximal PKA-stimulated lipolysis. In the absence of PKA site 5,

the phosphorylation of other serine residues in PKA sites of perilipin A increases

lipolysis to a significant extent. Importantly, we propose that the phosphorylation of serine 492 mediates ATGL-catalyzed lipolysis through a general mechanism that does not depend on the availability of CGI-58. In the presence of CGI-58, the perilipin A-mediated binding and dispersion of CGI-58 from lipid droplets under basal and stimulated conditions, respectively, is an additional mechanism for the control of ATGL-mediated lipolysis. Further studies directed to understand the underlying details of this general mechanism will provide new insights into the events that control lipid homeostasis in adipose tissue.

REFERENCES

1. Shi, Y., and Burn, P. (2004). Lipid metabolic enzymes: emerging drug targets for the treatment of obesity. *Nat Rev Drug Discov* **3**, 695-710

2. Cawley, J., and Meyerhoefer, C. (2012). The medical care costs of obesity: an instrumental variables approach. *J Health Econ* **31**, 219-230

3. Walther, T. C., and Farese, R. V., Jr. (2012). Lipid droplets and cellular lipid metabolism. *Annu Rev Biochem* **81**, 687-714

4. Murphy, D. J. (2001). The biogenesis and functions of lipid bodies in animals, plants and microorganisms. *Prog Lipid Res* **40**, 325-438

5. Guo, Y., Cordes, K. R., Farese, R. V., Jr., and Walther, T. C. (2009). Lipid droplets at a glance. *J Cell Sci* **122**, 749-752

6. Schaffer, J. E. (2003). Lipotoxity: when tissues overeat. *Curr Opin Lipidol* **14**, 281-287

7. Brasaemle, D. L., Rubin, B., Harten, I. A., Gruia-Gray, J., Kimmel, A. R., and Londos, C. (2000). Perilipin A increases triacylglycerol storage by decreasing the rate of triacylglycerol hydrolysis. *J Biol Chem* **275**, 38486-38493

8. Brasaemle, D. L. (2007). Thematic review series: adipocyte biology. The perilipin family of structural lipid droplet proteins: stabilization of lipid droplets and control of lipolysis. *J Lipid Res* **48**, 2547-2559

9. Subramanian, V., Rothenberg, A., Gomez, C., Cohen, A. W., Garcia, A., Bhattacharyya, S., Shapiro, L., Dolios, G., Wang, R., Lisanti, M. P., and Brasaemle, D. L. (2004). Perilipin A mediates the reversible binding of CGI-58 to lipid droplets in 3T3-L1 adipocytes. *J Biol Chem* **279**, 42062-42071

10. Granneman, J. G., Moore, H. P., Krishnamoorthy, R., and Rathod, M. (2009). Perilipin controls lipolysis by regulating the interactions of AB-hydrolase containing 5 (Abhd5) and adipose triglyceride lipase (Atgl). *J Biol Chem* **284**, 34538-34544

11. Bickel, P. E., Tansey, J. T., and Welte, M. A. (2009). PAT proteins, an ancient family of lipid droplet proteins that regulate cellular lipid stores. *Biochim Biophys Acta* **1791**, 419-440

12. Honnor, R. C., Dhillon, G. S., and Londos, C. (1985). cAMP-dependent protein kinase and lipolysis in rat adipocytes. II. Definition of steady-state relationship with lipolytic and antilipolytic modulators. *J Biol Chem* **260**, 15130-15138

13. Lampidonis, A. D., Rogdakis, E., Voutsinas, G. E., and Stravopodis, D. J. (2011). The resurgence of Hormone-Sensitive Lipase (HSL) in mammalian lipolysis. *Gene* **477**, 1-11

14. Greenberg, A. S., Egan, J. J., Wek, S. A., Garty, N. B., Blanchette-Mackie, E. J., and Londos, C. (1991). Perilipin, a major hormonally regulated adipocyte-specific phosphoprotein associated with the periphery of lipid storage droplets. *J Biol Chem* **266**, 11341-11346

15. Anthonsen, M. W., Ronnstrand, L., Wernstedt, C., Degerman, E., and Holm, C. (1998). Identification of novel phosphorylation sites in hormone-sensitive lipase that are phosphorylated in response to isoproterenol and govern activation properties in vitro. *J Biol Chem* **273**, 215-221

16. Brasaemle, D. L., Levin, D. M., Adler-Wailes, D. C., and Londos, C. (2000). The lipolytic stimulation of 3T3-L1 adipocytes promotes the translocation of hormone-sensitive lipase to the surfaces of lipid storage droplets. *Biochim Biophys Acta* **1483**, 251-262

17. Sztalryd, C., Xu, G., Dorward, H., Tansey, J. T., Contreras, J. A., Kimmel, A. R., and Londos, C. (2003). Perilipin A is essential for the translocation of hormone-sensitive lipase during lipolytic activation. *J Cell Biol* **161**, 1093-1103

18. Granneman, J. G., Moore, H. P., Granneman, R. L., Greenberg, A. S., Obin, M. S., and Zhu, Z. (2007). Analysis of lipolytic protein trafficking and interactions in adipocytes. *J Biol Chem* **282**, 5726-5735

19. Wang, H., Bell, M., Sreenivasan, U., Hu, H., Liu, J., Dalen, K., Londos, C., Yamaguchi, T., Rizzo, M. A., Coleman, R., Gong, D., Brasaemle, D., and Sztalryd, C. (2011). Unique regulation of adipose triglyceride lipase (ATGL) by perilipin 5, a lipid droplet-associated protein. *J Biol Chem* **286**, 15707-15715

20. Haemmerle, G., Zimmermann, R., Hayn, M., Theussl, C., Waeg, G., Wagner, E., Sattler, W., Magin, T. M., Wagner, E. F., and Zechner, R. (2002). Hormone-sensitive lipase deficiency in mice causes diglyceride accumulation in adipose tissue, muscle, and testis. *J Biol Chem* **277**, 4806-4815

21. Schweiger, M., Schreiber, R., Haemmerle, G., Lass, A., Fledelius, C., Jacobsen, P., Tornqvist, H., Zechner, R., and Zimmermann, R. (2006). Adipose triglyceride lipase and hormone-sensitive lipase are the major enzymes in adipose tissue triacylglycerol catabolism. *J Biol Chem* **281**, 40236-40241

22. Bezaire, V., Mairal, A., Ribet, C., Lefort, C., Girousse, A., Jocken, J., Laurencikiene, J., Anesia, R., Rodriguez, A. M., Ryden, M., Stenson, B. M., Dani, C., Ailhaud, G., Arner, P., and Langin, D. (2009). Contribution of adipose triglyceride lipase and hormone-sensitive lipase to lipolysis in hMADS adipocytes. *J Biol Chem* **284**, 18282-18291

23. Fredrikson, G., Tornqvist, H., and Belfrage, P. (1986). Hormone-sensitive lipase and monoacylglycerol lipase are both required for complete degradation of adipocyte triacylglycerol. *Biochim Biophys Acta* **876**, 288-293

24. Holm, C. (2003). Molecular mechanisms regulating hormone-sensitive lipase and lipolysis. *Biochem Soc Trans* **31**, 1120-1124

25. Egan, J. J., Greenberg, A. S., Chang, M. K., and Londos, C. (1990). Control of endogenous phosphorylation of the major cAMP-dependent protein kinase substrate in adipocytes by insulin and beta-adrenergic stimulation. *J Biol Chem* **265**, 18769-18775

26. Kimmel, A. R., Brasaemle, D. L., McAndrews-Hill, M., Sztalryd, C., and Londos, C. (2010). Adoption of PERILIPIN as a unifying nomenclature for the mammalian PAT-family of intracellular lipid storage droplet proteins. *J Lipid Res* **51**, 468-471

27. Greenberg, A. S., Egan, J. J., Wek, S. A., Moos, M. C., Jr., Londos, C., and Kimmel, A. R. (1993). Isolation of cDNAs for perilipins A and B: sequence and expression of lipid droplet-associated proteins of adipocytes. *Proc Natl Acad Sci U S A* **90**, 12035-12039

28. Lu, X., Gruia-Gray, J., Copeland, N. G., Gilbert, D. J., Jenkins, N. A., Londos, C., and Kimmel, A. R. (2001). The murine perilipin gene: the lipid droplet-associated

perilipins derive from tissue-specific, mRNA splice variants and define a gene family of ancient origin. *Mamm Genome* **12**, 741-749

29. Blanchette-Mackie, E. J., Dwyer, N. K., Barber, T., Coxey, R. A., Takeda, T., Rondinone, C. M., Theodorakis, J. L., Greenberg, A. S., and Londos, C. (1995). Perilipin is located on the surface layer of intracellular lipid droplets in adipocytes. *J Lipid Res* **36**, 1211-1226

30. Servetnick, D. A., Brasaemle, D. L., Gruia-Gray, J., Kimmel, A. R., Wolff, J., and Londos, C. (1995). Perilipins are associated with cholesteryl ester droplets in steroidogenic adrenal cortical and Leydig cells. *J Biol Chem* **270**, 16970-16973

31. Garcia, A., Sekowski, A., Subramanian, V., and Brasaemle, D. L. (2003). The central domain is required to target and anchor perilipin A to lipid droplets. *J Biol Chem* **278**, 625-635

32. Subramanian, V., Garcia, A., Sekowski, A., and Brasaemle, D. L. (2004). Hydrophobic sequences target and anchor perilipin A to lipid droplets. *J Lipid Res* **45**, 1983-1991

33. Garcia, A., Subramanian, V., Sekowski, A., Bhattacharyya, S., Love, M. W., and Brasaemle, D. L. (2004). The amino and carboxyl termini of perilipin a facilitate the storage of triacylglycerols. *J Biol Chem* **279**, 8409-8416

34. Brasaemle, D. L., Barber, T., Kimmel, A. R., and Londos, C. (1997). Post-translational regulation of perilipin expression. Stabilization by stored intracellular neutral lipids. *J Biol Chem* **272**, 9378-9387

35. Kovsan, J., Ben-Romano, R., Souza, S. C., Greenberg, A. S., and Rudich, A. (2007). Regulation of adipocyte lipolysis by degradation of the perilipin protein: nelfinavir enhances lysosome-mediated perilipin proteolysis. *J Biol Chem* **282**, 21704-21711

36. Xu, G., Sztalryd, C., and Londos, C. (2006). Degradation of perilipin is mediated through ubiquitination-proteasome pathway. *Biochim Biophys Acta* **1761**, 83-90

37. Souza, S. C., de Vargas, L. M., Yamamoto, M. T., Lien, P., Franciosa, M. D., Moss, L. G., and Greenberg, A. S. (1998). Overexpression of perilipin A and B blocks the ability of tumor necrosis factor alpha to increase lipolysis in 3T3-L1 adipocytes. *J Biol Chem* **273**, 24665-24669

38. Martinez-Botas, J., Anderson, J. B., Tessier, D., Lapillonne, A., Chang, B. H., Quast, M. J., Gorenstein, D., Chen, K. H., and Chan, L. (2000). Absence of perilipin results in leanness and reverses obesity in Lepr(db/db) mice. *Nat Genet* **26**, 474-479

39. Tansey, J. T., Sztalryd, C., Gruia-Gray, J., Roush, D. L., Zee, J. V., Gavrilova, O., Reitman, M. L., Deng, C. X., Li, C., Kimmel, A. R., and Londos, C. (2001). Perilipin ablation results in a lean mouse with aberrant adipocyte lipolysis, enhanced leptin production, and resistance to diet-induced obesity. *Proc Natl Acad Sci U S A* **98**, 6494-6499

40. Zhang, H. H., Souza, S. C., Muliro, K. V., Kraemer, F. B., Obin, M. S., and Greenberg, A. S. (2003). Lipase-selective functional domains of perilipin A differentially regulate constitutive and protein kinase A-stimulated lipolysis. *J Biol Chem* **278**, 51535-51542

41. Wang, H., Hu, L., Dalen, K., Dorward, H., Marcinkiewicz, A., Russell, D., Gong, D., Londos, C., Yamaguchi, T., Holm, C., Rizzo, M. A., Brasaemle, D., and

Sztalryd, C. (2009). Activation of hormone-sensitive lipase requires two steps, protein phosphorylation and binding to the PAT-1 domain of lipid droplet coat proteins. *J Biol Chem* **284**, 32116-32125

42. Miyoshi, H., Perfield, J. W., 2nd, Souza, S. C., Shen, W. J., Zhang, H. H., Stancheva, Z. S., Kraemer, F. B., Obin, M. S., and Greenberg, A. S. (2007). Control of adipose triglyceride lipase action by serine 517 of perilipin A globally regulates protein kinase A-stimulated lipolysis in adipocytes. *J Biol Chem* **282**, 996-1002

43. Jiang, H. P., and Serrero, G. (1992). Isolation and characterization of a full-length cDNA coding for an adipose differentiation-related protein. *Proc Natl Acad Sci U S A* **89**, 7856-7860

44. Brasaemle, D. L., Barber, T., Wolins, N. E., Serrero, G., Blanchette-Mackie, E. J., and Londos, C. (1997). Adipose differentiation-related protein is an ubiquitously expressed lipid storage droplet-associated protein. *J Lipid Res* **38**, 2249-2263

45. Xu, G., Sztalryd, C., Lu, X., Tansey, J. T., Gan, J., Dorward, H., Kimmel, A. R., and Londos, C. (2005). Post-translational regulation of adipose differentiation-related protein by the ubiquitin/proteasome pathway. *J Biol Chem* **280**, 42841-42847

46. Gao, J., and Serrero, G. (1999). Adipose differentiation related protein (ADRP) expressed in transfected COS-7 cells selectively stimulates long chain fatty acid uptake. *J Biol Chem* **274**, 16825-16830

47. Larigauderie, G., Cuaz-Perolin, C., Younes, A. B., Furman, C., Lasselin, C., Copin, C., Jaye, M., Fruchart, J. C., and Rouis, M. (2006). Adipophilin increases triglyceride storage in human macrophages by stimulation of biosynthesis and inhibition of beta-oxidation. *FEBS J* **273**, 3498-3510

48. Imamura, M., Inoguchi, T., Ikuyama, S., Taniguchi, S., Kobayashi, K., Nakashima, N., and Nawata, H. (2002). ADRP stimulates lipid accumulation and lipid droplet formation in murine fibroblasts. *Am J Physiol Endocrinol Metab* **283**, E775-783

49. Listenberger, L. L., Ostermeyer-Fay, A. G., Goldberg, E. B., Brown, W. J., and Brown, D. A. (2007). Adipocyte differentiation-related protein reduces the lipid droplet association of adipose triglyceride lipase and slows triacylglycerol turnover. *J Lipid Res* **48**, 2751-2761

50. Tansey, J. T., Huml, A. M., Vogt, R., Davis, K. E., Jones, J. M., Fraser, K. A., Brasaemle, D. L., Kimmel, A. R., and Londos, C. (2003). Functional studies on native and mutated forms of perilipins. A role in protein kinase A-mediated lipolysis of triacylglycerols. *J Biol Chem* **278**, 8401-8406

51. Chang, B. H., Li, L., Paul, A., Taniguchi, S., Nannegari, V., Heird, W. C., and Chan, L. (2006). Protection against fatty liver but normal adipogenesis in mice lacking adipose differentiation-related protein. *Mol Cell Biol* **26**, 1063-1076

52. Russell, T. D., Palmer, C. A., Orlicky, D. J., Bales, E. S., Chang, B. H., Chan, L., and McManaman, J. L. (2008). Mammary glands of adipophilin-null mice produce an amino-terminally truncated form of adipophilin that mediates milk lipid droplet formation and secretion. *J Lipid Res* **49**, 206-216

53. McManaman, J. L., Bales, E. S., Orlicky, D. J., Jackman, M., MacLean, P. S., Cain, S., Crunk, A. E., Mansur, A., Graham, C. E., Bowman, T. A., and

Greenberg, A. S. (2013). Perilipin-2-null mice are protected against diet-induced obesity, adipose inflammation, and fatty liver disease. *J Lipid Res* **54**, 1346-1359

54. Imai, Y., Varela, G. M., Jackson, M. B., Graham, M. J., Crooke, R. M., and Ahima, R. S. (2007). Reduction of hepatosteatosis and lipid levels by an adipose differentiation-related protein antisense oligonucleotide. *Gastroenterology* **132**, 1947-1954

55. Dalen, K. T., Dahl, T., Holter, E., Arntsen, B., Londos, C., Sztalryd, C., and Nebb, H. I. (2007). LSDP5 is a PAT protein specifically expressed in fatty acid oxidizing tissues. *Biochim Biophys Acta* **1771**, 210-227

56. Wolins, N. E., Quaynor, B. K., Skinner, J. R., Tzekov, A., Croce, M. A., Gropler, M. C., Varma, V., Yao-Borengasser, A., Rasouli, N., Kern, P. A., Finck, B. N., and Bickel, P. E. (2006). OXPAT/PAT-1 is a PPAR-induced lipid droplet protein that promotes fatty acid utilization. *Diabetes* **55**, 3418-3428

57. Yamaguchi, T., Matsushita, S., Motojima, K., Hirose, F., and Osumi, T. (2006). MLDP, a novel PAT family protein localized to lipid droplets and enriched in the heart, is regulated by peroxisome proliferator-activated receptor alpha. *J Biol Chem* **281**, 14232-14240

58. Diaz, E., and Pfeffer, S. R. (1998). TIP47: a cargo selection device for mannose 6-phosphate receptor trafficking. *Cell* **93**, 433-443

59. Wolins, N. E., Rubin, B., and Brasaemle, D. L. (2001). TIP47 associates with lipid droplets. *J Biol Chem* **276**, 5101-5108

60. Hickenbottom, S. J., Kimmel, A. R., Londos, C., and Hurley, J. H. (2004). Structure of a lipid droplet protein; the PAT family member TIP47. *Structure* **12**, 1199-1207

61. Hynson, R. M., Jeffries, C. M., Trewhella, J., and Cocklin, S. (2012). Solution structure studies of monomeric human TIP47/perilipin-3 reveal a highly extended conformation. *Proteins* **80**, 2046-2055

62. Hatters, D. M., Peters-Libeu, C. A., and Weisgraber, K. H. (2006). Apolipoprotein E structure: insights into function. *Trends Biochem Sci* **31**, 445-454

63. Wolins, N. E., Quaynor, B. K., Skinner, J. R., Schoenfish, M. J., Tzekov, A., and Bickel, P. E. (2005). S3-12, Adipophilin, and TIP47 package lipid in adipocytes. *J Biol Chem* **280**, 19146-19155

64. Sztalryd, C., Bell, M., Lu, X., Mertz, P., Hickenbottom, S., Chang, B. H., Chan, L., Kimmel, A. R., and Londos, C. (2006). Functional compensation for adipose differentiation-related protein (ADFP) by Tip47 in an ADFP null embryonic cell line. *J Biol Chem* **281**, 34341-34348

65. Bell, M., Wang, H., Chen, H., McLenithan, J. C., Gong, D. W., Yang, R. Z., Yu, D., Fried, S. K., Quon, M. J., Londos, C., and Sztalryd, C. (2008). Consequences of lipid droplet coat protein downregulation in liver cells: abnormal lipid droplet metabolism and induction of insulin resistance. *Diabetes* **57**, 2037-2045

66. Scherer, P. E., Bickel, P. E., Kotler, M., and Lodish, H. F. (1998). Cloning of cell-specific secreted and surface proteins by subtractive antibody screening. *Nat Biotechnol* **16**, 581-586

67. Wolins, N. E., Skinner, J. R., Schoenfish, M. J., Tzekov, A., Bensch, K. G., and Bickel, P. E. (2003). Adipocyte protein S3-12 coats nascent lipid droplets. *J Biol Chem* **278**, 37713-37721

68. Bussell, R., Jr., and Eliezer, D. (2003). A structural and functional role for 11-mer repeats in alpha-synuclein and other exchangeable lipid binding proteins. *J Mol Biol* **329**, 763-778

69. Granneman, J. G., Moore, H. P., Mottillo, E. P., Zhu, Z., and Zhou, L. (2011). Interactions of perilipin-5 (Plin5) with adipose triglyceride lipase. *J Biol Chem* **286**, 5126-5135

70. Vaughan, M., Berger, J. E., and Steinberg, D. (1964). Hormone-Sensitive Lipase and Monoglyceride Lipase Activities in Adipose Tissue. *J Biol Chem* **239**, 401-409

71. Fredrikson, G., Stralfors, P., Nilsson, N. O., and Belfrage, P. (1981). Hormone-sensitive lipase of rat adipose tissue. Purification and some properties. *J Biol Chem* **256**, 6311-6320

72. Holm, C., Kirchgessner, T. G., Svenson, K. L., Fredrikson, G., Nilsson, S., Miller, C. G., Shively, J. E., Heinzmann, C., Sparkes, R. S., Mohandas, T., and et al. (1988). Hormone-sensitive lipase: sequence, expression, and chromosomal localization to 19 cent-q13.3. *Science* **241**, 1503-1506

73. Kraemer, F. B., Patel, S., Saedi, M. S., and Sztalryd, C. (1993). Detection of hormone-sensitive lipase in various tissues. I. Expression of an HSL/bacterial fusion protein and generation of anti-HSL antibodies. *J Lipid Res* **34**, 663-671

74. Small, C. A., Garton, A. J., and Yeaman, S. J. (1989). The presence and role of hormone-sensitive lipase in heart muscle. *Biochem J* **258**, 67-72

75. Langfort, J., Ploug, T., Ihlemann, J., Enevoldsen, L. H., Stallknecht, B., Saldo, M., Kjaer, M., Holm, C., and Galbo, H. (1998). Hormone-sensitive lipase (HSL) expression and regulation in skeletal muscle. *Adv Exp Med Biol* **441**, 219-228

76. Contreras, J. A., Holm, C., Martin, A., Gaspar, M. L., and Lasuncion, M. A. (1994). Presence of hormone-sensitive lipase mRNA in J774 macrophages. *Isr J Med Sci* **30**, 778-781

77. Jepson, C. A., and Yeaman, S. J. (1993). Expression of hormone-sensitive lipase in macrophage foam cells. *Biochem Soc Trans* **21 (Pt 3)**, 232S

78. Klannemark, M., Orho, M., Langin, D., Laurell, H., Holm, C., Reynisdottir, S., Arner, P., and Groop, L. (1998). The putative role of the hormone-sensitive lipase gene in the pathogenesis of Type II diabetes mellitus and abdominal obesity. *Diabetologia* **41**, 1516-1522

79. Cook, K. G., Lee, F. T., and Yeaman, S. J. (1981). Hormone-sensitive cholesterol ester hydrolase of bovine adrenal cortex: identification of the enzyme protein. *FEBS Lett* **132**, 10-14

80. Wei, S., Lai, K., Patel, S., Piantedosi, R., Shen, H., Colantuoni, V., Kraemer, F. B., and Blaner, W. S. (1997). Retinyl ester hydrolysis and retinol efflux from BFC-1beta adipocytes. *J Biol Chem* **272**, 14159-14165

81. Belfrage, P., Fredrikson, G., Nilsson, N. O., and Stralfors, P. (1981). Regulation of adipose-tissue lipolysis by phosphorylation of hormone-sensitive lipase. *Int J Obes* **5**, 635-641

82. Shakur, Y., Holst, L. S., Landstrom, T. R., Movsesian, M., Degerman, E., and Manganiello, V. (2001). Regulation and function of the cyclic nucleotide phosphodiesterase (PDE3) gene family. *Prog Nucleic Acid Res Mol Biol* **66**, 241-277

83. Su, C. L., Sztalryd, C., Contreras, J. A., Holm, C., Kimmel, A. R., and Londos, C. (2003). Mutational analysis of the hormone-sensitive lipase translocation reaction in adipocytes. *J Biol Chem* **278**, 43615-43619

84. Egan, J. J., Greenberg, A. S., Chang, M. K., Wek, S. A., Moos, M. C., Jr., and Londos, C. (1992). Mechanism of hormone-stimulated lipolysis in adipocytes: translocation of hormone-sensitive lipase to the lipid storage droplet. *Proc Natl Acad Sci U S A* **89**, 8537-8541

85. Miyoshi, H., Souza, S. C., Zhang, H. H., Strissel, K. J., Christoffolete, M. A., Kovsan, J., Rudich, A., Kraemer, F. B., Bianco, A. C., Obin, M. S., and Greenberg, A. S. (2006). Perilipin promotes hormone-sensitive lipase-mediated adipocyte lipolysis via phosphorylation-dependent and -independent mechanisms. *J Biol Chem* **281**, 15837-15844

86. Souza, S. C., Muliro, K. V., Liscum, L., Lien, P., Yamamoto, M. T., Schaffer, J. E., Dallal, G. E., Wang, X., Kraemer, F. B., Obin, M., and Greenberg, A. S. (2002). Modulation of hormone-sensitive lipase and protein kinase A-mediated lipolysis by perilipin A in an adenoviral reconstituted system. *J Biol Chem* **277**, 8267-8272

87. Osuga, J., Ishibashi, S., Oka, T., Yagyu, H., Tozawa, R., Fujimoto, A., Shionoiri, F., Yahagi, N., Kraemer, F. B., Tsutsumi, O., and Yamada, N. (2000). Targeted disruption of hormone-sensitive lipase results in male sterility and adipocyte hypertrophy, but not in obesity. *Proc Natl Acad Sci U S A* **97**, 787-792

88. Chung, S., Wang, S. P., Pan, L., Mitchell, G., Trasler, J., and Hermo, L. (2001). Infertility and testicular defects in hormone-sensitive lipase-deficient mice. *Endocrinology* **142**, 4272-4281

89. Zimmermann, R., Strauss, J. G., Haemmerle, G., Schoiswohl, G., Birner-Gruenberger, R., Riederer, M., Lass, A., Neuberger, G., Eisenhaber, F., Hermetter, A., and Zechner, R. (2004). Fat mobilization in adipose tissue is promoted by adipose triglyceride lipase. *Science* **306**, 1383-1386

90. Villena, J. A., Roy, S., Sarkadi-Nagy, E., Kim, K. H., and Sul, H. S. (2004). Desnutrin, an adipocyte gene encoding a novel patatin domain-containing protein, is induced by fasting and glucocorticoids: ectopic expression of desnutrin increases triglyceride hydrolysis. *J Biol Chem* **279**, 47066-47075

91. Jenkins, C. M., Mancuso, D. J., Yan, W., Sims, H. F., Gibson, B., and Gross, R. W. (2004). Identification, cloning, expression, and purification of three novel human calcium-independent phospholipase A2 family members possessing triacylglycerol lipase and acylglycerol transacylase activities. *J Biol Chem* **279**, 48968-48975

92. Wilson, P. A., Gardner, S. D., Lambie, N. M., Commans, S. A., and Crowther, D. J. (2006). Characterization of the human patatin-like phospholipase family. *J Lipid Res* **47**, 1940-1949

93. Lake, A. C., Sun, Y., Li, J. L., Kim, J. E., Johnson, J. W., Li, D., Revett, T., Shih, H. H., Liu, W., Paulsen, J. E., and Gimeno, R. E. (2005). Expression, regulation,

and triglyceride hydrolase activity of Adiponutrin family members. *J Lipid Res* **46**, 2477-2487

94. Haemmerle, G., Lass, A., Zimmermann, R., Gorkiewicz, G., Meyer, C., Rozman, J., Heldmaier, G., Maier, R., Theussl, C., Eder, S., Kratky, D., Wagner, E. F., Klingenspor, M., Hoefler, G., and Zechner, R. (2006). Defective lipolysis and altered energy metabolism in mice lacking adipose triglyceride lipase. *Science* **312**, 734-737

95. Ahmadian, M., Duncan, R. E., Varady, K. A., Frasson, D., Hellerstein, M. K., Birkenfeld, A. L., Samuel, V. T., Shulman, G. I., Wang, Y., Kang, C., and Sul, H. S. (2009). Adipose overexpression of desnutrin promotes fatty acid use and attenuates diet-induced obesity. *Diabetes* **58**, 855-866

96. Pagnon, J., Matzaris, M., Stark, R., Meex, R. C., Macaulay, S. L., Brown, W., O'Brien, P. E., Tiganis, T., and Watt, M. J. (2012). Identification and functional characterization of protein kinase A phosphorylation sites in the major lipolytic protein, adipose triglyceride lipase. *Endocrinology* **153**, 4278-4289

97. Lass, A., Zimmermann, R., Haemmerle, G., Riederer, M., Schoiswohl, G., Schweiger, M., Kienesberger, P., Strauss, J. G., Gorkiewicz, G., and Zechner, R. (2006). Adipose triglyceride lipase-mediated lipolysis of cellular fat stores is activated by CGI-58 and defective in Chanarin-Dorfman Syndrome. *Cell Metab* **3**, 309-319

98. Lu, X., Yang, X., and Liu, J. (2010). Differential control of ATGL-mediated lipid droplet degradation by CGI-58 and G0S2. *Cell Cycle* **9**, 2719-2725

99. Yang, X., Lu, X., Lombes, M., Rha, G. B., Chi, Y. I., Guerin, T. M., Smart, E. J., and Liu, J. (2010). The G(0)/G(1) switch gene 2 regulates adipose lipolysis through association with adipose triglyceride lipase. *Cell Metab* **11**, 194-205

100. Brasaemle, D. L., Dolios, G., Shapiro, L., and Wang, R. (2004). Proteomic analysis of proteins associated with lipid droplets of basal and lipolytically stimulated 3T3-L1 adipocytes. *J Biol Chem* **279**, 46835-46842

101. Yamaguchi, T., Omatsu, N., Matsushita, S., and Osumi, T. (2004). CGI-58 interacts with perilipin and is localized to lipid droplets. Possible involvement of CGI-58 mislocalization in Chanarin-Dorfman syndrome. *J Biol Chem* **279**, 30490-30497

102. Lai, C. H., Chou, C. Y., Ch'ang, L. Y., Liu, C. S., and Lin, W. (2000). Identification of novel human genes evolutionarily conserved in Caenorhabditis elegans by comparative proteomics. *Genome Res* **10**, 703-713

103. Lefevre, C., Jobard, F., Caux, F., Bouadjar, B., Karaduman, A., Heilig, R., Lakhdar, H., Wollenberg, A., Verret, J. L., Weissenbach, J., Ozguc, M., Lathrop, M., Prud'homme, J. F., and Fischer, J. (2001). Mutations in CGI-58, the gene encoding a new protein of the esterase/lipase/thioesterase subfamily, in Chanarin-Dorfman syndrome. *Am J Hum Genet* **69**, 1002-1012

104. Chanarin, I., Patel, A., Slavin, G., Wills, E. J., Andrews, T. M., and Stewart, G. (1975). Neutral-lipid storage disease: a new disorder of lipid metabolism. *Br Med J* **1**, 553-555

105. Dorfman, M. L., Hershko, C., Eisenberg, S., and Sagher, F. (1974). Ichthyosiform dermatosis with systemic lipidosis. *Arch Dermatol* **110**, 261-266

106. Williams, M. L., Coleman, R. A., Placezk, D., and Grunfeld, C. (1991). Neutral lipid storage disease: a possible functional defect in phospholipid- linked triacylglycerol metabolism. *Biochim Biophys Acta* **1096**, 162-169

107. Radner, F. P., Streith, I. E., Schoiswohl, G., Schweiger, M., Kumari, M., Eichmann, T. O., Rechberger, G., Koefeler, H. C., Eder, S., Schauer, S., Theussl, H. C., Preiss-Landl, K., Lass, A., Zimmermann, R., Hoefler, G., Zechner, R., and Haemmerle, G. (2010). Growth retardation, impaired triacylglycerol catabolism, hepatic steatosis, and lethal skin barrier defect in mice lacking comparative gene identification-58 (CGI-58). *J Biol Chem* **285**, 7300-7311

108. Bruno, C., Bertini, E., Di Rocco, M., Cassandrini, D., Ruffa, G., De Toni, T., Seri, M., Spada, M., Li Volti, G., D'Amico, A., Trucco, F., Arca, M., Casali, C., Angelini, C., Dimauro, S., and Minetti, C. (2008). Clinical and genetic characterization of Chanarin-Dorfman syndrome. *Biochem Biophys Res Commun* **369**, 1125-1128

109. Fischer, J., Lefevre, C., Morava, E., Mussini, J. M., Laforet, P., Negre-Salvayre, A., Lathrop, M., and Salvayre, R. (2007). The gene encoding adipose triglyceride lipase (PNPLA2) is mutated in neutral lipid storage disease with myopathy. *Nat Genet* **39**, 28-30

110. Londos, C., Brasaemle, D. L., Schultz, C. J., Segrest, J. P., and Kimmel, A. R. (1999). Perilipins, ADRP, and other proteins that associate with intracellular neutral lipid droplets in animal cells. *Semin Cell Dev Biol* **10**, 51-58

111. Granneman, J. G., Li, P., Zhu, Z., and Lu, Y. (2005). Metabolic and cellular plasticity in white adipose tissue I: effects of beta3-adrenergic receptor activation. *Am J Physiol Endocrinol Metab* **289**, E608-616

112. Marcinkiewicz, A., Gauthier, D., Garcia, A., and Brasaemle, D. L. (2006). The phosphorylation of serine 492 of perilipin a directs lipid droplet fragmentation and dispersion. *J Biol Chem* **281**, 11901-11909

113. Ariotti, N., Murphy, S., Hamilton, N. A., Wu, L., Green, K., Schieber, N. L., Li, P., Martin, S., and Parton, R. G. (2012). Postlipolytic insulin-dependent remodeling of micro lipid droplets in adipocytes. *Mol Biol Cell* **23**, 1826-1837

114. Orlicky, D. J., DeGregori, J., and Schaack, J. (2001). Construction of stable coxsackievirus and adenovirus receptor-expressing 3T3-L1 cells. *J Lipid Res* **42**, 910-915

115. Paar, M., Jungst, C., Steiner, N. A., Magnes, C., Sinner, F., Kolb, D., Lass, A., Zimmermann, R., Zumbusch, A., Kohlwein, S. D., and Wolinski, H. (2012). Remodeling of lipid droplets during lipolysis and growth in adipocytes. *J Biol Chem* **287**, 11164-11173

116. Hashimoto, T., Segawa, H., Okuno, M., Kano, H., Hamaguchi, H. O., Haraguchi, T., Hiraoka, Y., Hasui, S., Yamaguchi, T., Hirose, F., and Osumi, T. (2012). Active involvement of micro-lipid droplets and lipid-droplet-associated proteins in hormone-stimulated lipolysis in adipocytes. *J Cell Sci* **125**, 6127-6136

117. Gocze, P. M., and Freeman, D. A. (1994). Factors underlying the variability of lipid droplet fluorescence in MA-10 Leydig tumor cells. *Cytometry* **17**, 151-158

118. Schultz, C. J., Torres, E., Londos, C., and Torday, J. S. (2002). Role of adipocyte differentiation-related protein in surfactant phospholipid synthesis by type II cells. *Am J Physiol Lung Cell Mol Physiol* **283**, L288-296

119. Jager, L., Hausl, M. A., Rauschhuber, C., Wolf, N. M., Kay, M. A., and Ehrhardt, A. (2009). A rapid protocol for construction and production of high-capacity adenoviral vectors. *Nat Protoc* **4**, 547-564

120. Schwartz, D. M., and Wolins, N. E. (2007). A simple and rapid method to assay triacylglycerol in cells and tissues. *J Lipid Res* **48**, 2514-2520

121. Bligh, E. G., and Dyer, W. J. (1959). A rapid method of total lipid extraction and purification. *Can J Biochem Physiol* **37**, 911-917

122. Laemmli, U. K. (1970). Cleavage of structural proteins during the assembly of the head of bacteriophage T4. *Nature* **227**, 680-685

123. Tarrant, M. K., and Cole, P. A. (2009). The chemical biology of protein phosphorylation. *Annu Rev Biochem* **78**, 797-825

124. Kanshin, E., Wang, S., Ashmarina, L., Fedjaev, M., Nifant'ev, I., Mitchell, G. A., and Pshezhetsky, A. V. (2009). The stoichiometry of protein phosphorylation in adipocyte lipid droplets: analysis by N-terminal isotope tagging and enzymatic dephosphorylation. *Proteomics* **9**, 5067-5077

125. Huttlin, E. L., Jedrychowski, M. P., Elias, J. E., Goswami, T., Rad, R., Beausoleil, S. A., Villen, J., Haas, W., Sowa, M. E., and Gygi, S. P. (2010). A tissue-specific atlas of mouse protein phosphorylation and expression. *Cell* **143**, 1174-1189

126. Humphrey, S. J., Yang, G., Yang, P., Fazakerley, D. J., Stockli, J., Yang, J. Y., and James, D. E. (2013). Dynamic adipocyte phosphoproteome reveals that Akt directly regulates mTORC2. *Cell Metab* **17**, 1009-1020

127. Gandotra, S., Le Dour, C., Bottomley, W., Cervera, P., Giral, P., Reznik, Y., Charpentier, G., Auclair, M., Delepine, M., Barroso, I., Semple, R. K., Lathrop, M., Lascols, O., Capeau, J., O'Rahilly, S., Magre, J., Savage, D. B., and Vigouroux, C. (2011). Perilipin deficiency and autosomal dominant partial lipodystrophy. *N Engl J Med* **364**, 740-748

128. Gandotra, S., Lim, K., Girousse, A., Saudek, V., O'Rahilly, S., and Savage, D. B. (2011). Human frame shift mutations affecting the carboxyl terminus of perilipin increase lipolysis by failing to sequester the adipose triglyceride lipase (ATGL) coactivator AB-hydrolase-containing 5 (ABHD5). *J Biol Chem* **286**, 34998-35006